



THE UNIVERSITY *of* EDINBURGH

## Edinburgh Research Explorer

### Genetic diversity in the Andes

**Citation for published version:**

Gómez-Gutiérrez, MC, Pennington, RT, Neaves, LE, Milne, RI, Madriñán, S & Richardson, JE 2017, 'Genetic diversity in the Andes: variation within and between the South American species of *Oreobolus* R. Br. (Cyperaceae)' *Alpine Botany*, vol. 127, no. 2, pp. 155-170. DOI: 10.1007/s00035-017-0192-z

**Digital Object Identifier (DOI):**

[10.1007/s00035-017-0192-z](https://doi.org/10.1007/s00035-017-0192-z)

**Link:**

[Link to publication record in Edinburgh Research Explorer](#)

**Document Version:**

Peer reviewed version

**Published In:**

Alpine Botany

**Publisher Rights Statement:**

© Swiss Botanical Society 2017 The final publication is available at [link.springer.com](http://link.springer.com) via <http://dx.doi.org/10.1007/s00035-017-0192-z>

**General rights**

Copyright for the publications made accessible via the Edinburgh Research Explorer is retained by the author(s) and / or other copyright owners and it is a condition of accessing these publications that users recognise and abide by the legal requirements associated with these rights.

**Take down policy**

The University of Edinburgh has made every reasonable effort to ensure that Edinburgh Research Explorer content complies with UK legislation. If you believe that the public display of this file breaches copyright please contact [openaccess@ed.ac.uk](mailto:openaccess@ed.ac.uk) providing details, and we will remove access to the work immediately and investigate your claim.



[Click here to view linked References](#)

1  
2  
3  
4 **1 GENETIC DIVERSITY IN THE ANDES:**  
5  
6 **2 VARIATION WITHIN AND BETWEEN THE**  
7  
8 **3 SOUTH AMERICAN SPECIES OF *OREOBOLUS***  
9  
10 **4 R. Br. (CYPERACEAE)**

16 5 María Camila Gómez-Gutiérrez<sup>1,2</sup>, R. Toby Pennington<sup>1</sup>, Linda E. Neaves<sup>1,3</sup>, Richard  
17  
18 6 I. Milne<sup>2</sup>, Santiago Madriñán<sup>4</sup> and James E. Richardson<sup>1,5,†</sup>  
19  
20

22 7 <sup>1</sup> Tropical Diversity Section, Royal Botanic Garden Edinburgh, 20A Inverleith Row,  
23  
24 8 Edinburgh, EH3 5LR, United Kingdom  
25  
26

28 9 <sup>2</sup> Institute of Molecular Plant Sciences, School of Biological Sciences, The  
29  
30 10 University of Edinburgh, Daniel Rutherford Building, The King's Buildings,  
31  
32 11 Edinburgh, EH9 3BF, United Kingdom.  
33  
34  
35

36 12 <sup>3</sup> Australian Centre for Wildlife Genomics, Australian Museum Research Institute,  
37  
38 13 Australian Museum, 1 William Street, Sydney 2010, Australia.  
39  
40

42 14 <sup>4</sup> Laboratorio de Botánica y Sistemática, Departamento de Ciencias Biológicas,  
43  
44 15 Universidad de los Andes, Carrera 1 No. 18A – 10, Bogotá, Colombia.  
45  
46

48 16 <sup>5</sup> Programa de Biología, Universidad del Rosario, Carrera 26 No. 63B – 48, Bogotá,  
49  
50 17 Colombia.  
51

53 18 † Corresponding author, email: jamese.richardson@urosario.edu.co  
54  
55  
56  
57  
58  
59  
60  
61  
62  
63  
64  
65

19 ABSTRACT

1  
2  
3 20 This study examines genetic relationships among and within the South American  
4  
5 21 species of *Oreobolus* that span the temperate and tropical Andes hotspots and  
6  
7 22 represent a good case study to investigate diversification in the Páramo. A total of  
8  
9  
10 23 197 individuals covering the distributional range of most of these species were  
11  
12 24 sequenced for the nuclear ribosomal internal transcribed spacer (ITS) and 118  
13  
14 25 individuals for three chloroplast DNA regions (*trnL-F*, *trnH-psbA* and *rpl32-trnL*).  
15  
16 26 Haplotype networks and measures of genetic diversity were calculated at different  
17  
18 27 taxonomic and geographic levels. To test for possible geographic structure, a Spatial  
19  
20 28 Analysis of Molecular Variance (SAMOVA) was undertaken and species  
21  
22 29 relationships were recovered using a coalescent-based approach. Results indicate  
23  
24 30 complex relationships among the five South American species of *Oreobolus*, which  
25  
26 31 are likely to have been confounded by incomplete lineage sorting, though  
27  
28 32 hybridization cannot be completely discarded as an influence on genetic patterns,  
29  
30 33 particularly among the northern populations of *O. obtusangulus* and *O. cleefii*. We  
31  
32 34 report a case of cryptic speciation in *O. obtusangulus* where northern and southern  
33  
34 35 populations of morphologically similar individuals are genetically distinct in all  
35  
36 36 analyses. At the population level, the genetic evidence is consistent with contraction  
37  
38 37 and expansion of islands of Páramo vegetation during the climatic fluctuations of the  
39  
40 38 Quaternary, highlighting the role of these processes in shaping modern diversity in  
41  
42 39 that ecosystem.  
43  
44  
45  
46  
47  
48  
49  
50  
51  
52  
53  
54  
55  
56  
57  
58  
59  
60  
61  
62  
63  
64  
65

40 KEYWORDS

41 Biogeography, Andes, species tree, lineage sorting, hybridization, Páramo.

42 ACKNOWLEDGEMENTS

43 This work was funded by a School of Biological Sciences Scholarship provided  
44 through The University of Edinburgh. We thank the herbaria at Aarhus University,  
45 (Denmark), Naturalis (The Netherlands) and Reading University (Great Britain) for  
46 making material available for DNA extraction. We also thank three anonymous  
47 reviewers for their valuable comments and James Nicholls from The University of  
48 Edinburgh for assistance with the \*BEAST analysis.

49 INTRODUCTION

50 The Páramo is a putatively young ecosystem that appeared following the final uplift  
51 of the northern section of the Andes Mountain Range during the Pliocene, c. 5  
52 million years ago – Ma (van der Hammen 1974; van der Hammen and Cleef 1986;  
53 Hooghiemstra et al. 2006; Graham 2009). It occupies an area of 37500 km<sup>2</sup> and is  
54 distributed in a series of sky islands with c. 4000 plant species of which 60% are  
55 endemic (Lutelyn 1999; Buytaert et al. 2010). It has been proposed that the glacial-  
56 interglacial cycles of the Quaternary may have played an important role in shaping  
57 Páramo plant populations (van der Hammen 1974; Simpson 1975). The continuous  
58 contraction and expansion of altitudinal vegetation belts may have promoted the

59 contact of Páramo islands during glacial periods, enabling the migration and  
60 exchange of otherwise isolated taxa (van der Hammen and Cleef 1986). Conversely,  
61 during interglacial periods, Páramo islands may have been isolated, promoting  
62 speciation (van der Hammen and Cleef 1986). Furthermore, previous studies have  
63 demonstrated that Páramo lineages have significantly higher speciation rates than  
64 any other biodiversity hotspot on Earth and that many speciation events occurred  
65 during the Pleistocene (Madríñán et al. 2013). Recent divergence times among  
66 Páramo plant lineages might have implications, both at the phenotypic and genotypic  
67 level, because morphological diversity and differentiation may not reflect complete  
68 genetic divergence between and within closely related taxa (Schaal et al. 1998).

69 The five South American species of the schoenoid sedge *Oreobolus* R. Br. (*O. cleefii*  
70 L.E. Mora, *O. ecuadorensis* T. Koyama, *O. goeppingeri* Suess., *O. obtusangulus*  
71 Gaudich. and *O. venezuelensis* Steyerm.) are an ideal model system to investigate  
72 how recent climatic and/or geological events may have shaped extant populations in  
73 the Páramo. Previous studies have supported the monophyly of the South American  
74 clade of *Oreobolus* and dated its divergence to c. 5 Ma, coinciding with the  
75 appearance of the Páramo ecosystem (Chacón et al. 2006). The South American  
76 clade of *Oreobolus* is therefore a good exemplar to study Páramo biogeography,  
77 including investigating the likely effects of recent climatic events (i.e. glacial cycles  
78 of the Quaternary) on the population structure of its species.

79 A handful of genetic studies for similar high-altitude tropical ecosystems in Africa  
80 have been published in recent years (Kebede et al. 2007; Assefa et al. 2007; Gizaw et  
81 al. 2013; Kadu et al. 2013; Wondimu et al. 2013). However, such studies are almost  
82 non-existent for the Páramo flora (Vásquez et al. 2016; Kolář et al. 2016). The aims

83 of this study are to estimate the species phylogeny of the South American species of  
84 *Oreobolus* and their timing of diversification, to assess genetic structure at the inter-  
85 and intra-specific level and to interpret these in the light of Quaternary glacial-  
86 interglacial cycles.

## 87 METHODS

### 88 Study species and sampling

89 The species concepts for *Oreobolus* that we use here follow the monograph of  
90 Seberg (1988) for *O. ecuadorensis*, *O. goeppingeri*, *O. obtusangulus* and *O.*  
91 *venezuelensis*, and of Mora-Osejo (1987) for *O. cleefii*. These species, with the  
92 exception of *O. obtusangulus* subsp. *obtusangulus*, are restricted to wet, temperate-  
93 like environments in the northern section of the Tropical Andes and in the  
94 Talamanca Cordillera in southern Central America, and are found only in the high-  
95 altitude Páramo ecosystem (Seberg 1988; Chacón et al. 2006). *Oreobolus cleefii* is  
96 restricted to the Eastern Cordillera and the southern Andean region of Colombia.  
97 *Oreobolus ecuadorensis* is found in southern Colombia, Ecuador and northern Peru.  
98 *Oreobolus goeppingeri* is distributed in the Talamanca Cordillera in southern Central  
99 America, Colombia and Ecuador. *Oreobolus obtusangulus* has two subspecies with a  
100 disjunct distribution: subsp. *unispicus* is distributed in Colombia, Ecuador and  
101 northern Peru while subsp. *obtusangulus* occupies the subantarctic region of Chile,  
102 Argentina and the Falkland Islands. Finally, *O. venezuelensis* occupies all Páramo  
103 regions (Talamanca Cordillera, Venezuela, Colombia, Ecuador and northern Peru).

104 The distributions of all *Oreobolus* Páramo species overlap with those of at least one  
105 other congeneric species (Fig. 1). All Páramo species are found between 3000 and  
106 4300 m a.s.l. while in the subantarctic regions, the altitude at which *O. obtusangulus*  
107 is found decreases with increasing latitude, from 2400 m a.s.l. to sea level (Seberg  
108 1988). The five South American species are clearly differentiated in terms of  
109 morphology and, in common with most Cyperaceae, *Oreobolus* is both wind  
110 pollinated and dispersed (Seberg 1988). Little is known about ploidy levels and  
111 chromosome numbers in *Oreobolus*, with the only chromosome count for *O.*  
112 *obtusangulus* ssp. *obtusangulus* ( $2n = 48$ ; Moore (1967)).

113 The five South American species of *Oreobolus* (*O. cleefii*, *O. ecuadorensis*, *O.*  
114 *goeppingeri*, *O. obtusangulus* and *O. venezuelensis*) were sampled extensively across  
115 their entire distribution range (Fig. 1). A total of 269 samples from 32 sampling  
116 localities were obtained from both field collections (10 sampling localities) and  
117 herbarium material (22 sampling localities) (Fig. 1 and Supp. Table 1). From each of  
118 the ten field sampling localities, all within Colombia, two to ten fresh leaf samples  
119 per species were collected, and their location was recorded using a handheld GPS  
120 (Fig. 1, sampling localities 2 – 11). For sampling localities in Costa Rica, Ecuador,  
121 Peru, Chile and Argentina (Fig. 1, sampling localities 1 and 12 – 32), herbarium  
122 material was acquired from the Utrecht (U) and Leiden University (L) branches of  
123 the National Herbarium of the Netherlands, Aarhus University Herbarium (AAU)  
124 and the University of Reading Herbarium (RNG). For herbarium specimens, between  
125 one and ten individuals per species were sampled from each sampling locality.  
126 Coordinates were recorded from the herbarium specimens and checked for accuracy  
127 using the NGA GEOnet Names Server (GNS) (<http://geonames.nga.mil>). Sampling

128 localities are numbered 1 to 32 in a north to south direction. Sampling localities 1 to  
129 23 will be referred to as northern Andes – NA (Costa Rica, Colombia, Ecuador and  
130 Peru) and 24 to 32 as southern Andes – SA (Chile and Argentina). Previously  
131 published sequence data for *O. cleefii*, *O. goeppingeri* and *O. venezuelensis* (Chacón  
132 et al. 2006) were also incorporated and assigned to their corresponding sampling  
133 locality. Supplementary Table 2 presents the complete list of samples used in this  
134 study together with their GenBank numbers.

### 135 DNA extraction, amplification and sequencing

136 Both silica-dried fresh leaf samples and herbarium material were pulverised using a  
137 Mixer Mill (Retsch, Haan, Germany). Total genomic DNA from herbarium material  
138 was isolated following the CTAB method of Doyle and Doyle (1990) and from  
139 silica-dried samples with the DNeasy® Plant Mini Kit (QIAGEN, Manchester, UK)  
140 following the manufacturer's protocol. The chloroplast region *trnL-F* was amplified  
141 and sequenced using primers *trnLc* and *trnLf* for silica-dried material, and in  
142 combination with internal primers *trnLd* and *trnLe* for herbarium material (Taberlet  
143 et al. 1991). For silica-dried material, the ITS region was amplified and sequenced  
144 with external primers ITS5P and ITS8P (Möller and Cronk 1997). For herbarium  
145 material, owing to the increased likelihood of the DNA being degraded,  
146 amplification and sequencing were performed using external primers ITS5P and  
147 ITS8P in combination with internal primers ITS2P and ITS3P (Möller and Cronk  
148 1997), in order to amplify the shorter ITS1 and ITS2 regions in separate reactions.  
149 The chloroplast regions *trnH-psbA* and *rpl32-trnL* were amplified and sequenced  
150 using primer pairs *trnH*<sup>GUG</sup> (Tate and Simpson 2003)/*psbA* (Sang et al. 1997) and



151 *trnL*<sup>(UAG)</sup>/*rpl32*-F (Shaw et al. 2007), respectively. For all reactions, 20 µl PCR  
152 reactions used the following proportions: 1 µl of unquantified DNA, 1x Buffer  
153 (Bioline, London, UK), 1mM dNTPs, 1.5 mM MgCl<sub>2</sub> (Bioline, London, UK), 0.75  
154 µM of each forward and reverse primer, 4µl of combinatorial enhancer solution  
155 (CES) and 0.05 U of *Taq* polymerase (Bioline, London, UK). The amplification  
156 cycle for all chloroplast regions (*trnL*-F, *trnH-psbA* and *rpl32-trnL*) consisted of 2  
157 min at 94 °C, followed by 30 cycles of 1 min at 94 °C, 1 min at 52 °C and 1 min at 72  
158 °C, finalising with 7 min at 72 °C. For ITS, the amplification cycle consisted of 3 min  
159 at 94 °C, followed by 30 cycles of 1 min at 94 °C, 1 min at 55 °C and 90 sec at 72 °C,  
160 finalising with 5 min at 72 °C. PCR products were purified with 2 µl of ExoSAP-IT®  
161 (USB Corporation, High Wycombe, UK) for 5 µl of product. Sequencing reactions  
162 for each primer used the BigDye® Terminator v3.1 chemistry (Applied  
163 Biosystems™, Paisley, UK) and the manufacturer's protocol. Sequencing was  
164 performed at the Edinburgh Genomics facility of the University of Edinburgh. No  
165 double peaks were observed in the chromatograms of the ITS region and therefore it  
166 was not necessary to clone.

#### 167 Matrix assembly and sequence alignment

168 Contigs of forward and reverse sequences were assembled in Sequencher version 5.2  
169 (Gene Codes Corporation, Ann Arbor, Michigan, USA). 230 ITS sequences, 169  
170 *trnL*-F sequences, 128 *trnH-psbA* sequences and 190 *rpl32-trnL* sequences were  
171 generated for this study (Supp. Table 2). The sequences were manually aligned using  
172 Mesquite v2.75 (Maddison and Maddison 2014). Supplementary Table 3 describes

173 number of individuals successfully sequenced per species per cluster/sampling  
174 locality.

175 Species phylogeny and timing of diversification

176 The multispecies coalescent model implemented in \*BEAST 2 (Heled and  
177 Drummond 2012; Bouckaert et al. 2014) was used to estimate the phylogenetic  
178 relationships amongst the five South American species of *Oreobolus* as well as their  
179 divergence time. Only complete sequences were used for the species tree estimation  
180 (ITS, *trnL-F*, *trnH-psbA* and *rpl32-trnL*; Supp. Table 2). The analysis was run using  
181 bModelTest (Bouckaert and Drummond 2017) which is a model selection tool  
182 incorporated in BEAST 2 (Bouckaert et al. 2014) that uses a Bayesian framework  
183 (reversible jump MCMC) to select the most appropriate substitution model while  
184 simultaneously estimating the phylogeny. Phylogenetic reconstruction and  
185 divergence time estimations were performed using BEAST v2.4.5 (Bouckaert et al.  
186 2014). The tree model was linked for the three plastid regions because cpDNA does  
187 not undergo recombination. The model of lineage-specific substitution rate variation  
188 was set as a strict clock model for each dataset. A \*BEAST analysis requires each  
189 taxon to be associated with a species or taxonomic unit (Taxon Sets). These were  
190 defined following current taxonomy but with *O. obtusangulus* divided into northern  
191 and southern taxa (based upon results presented below). The diversification model  
192 for the species tree was set to a calibrated Yule model (Heled and Drummond 2012)  
193 with the population size model at its default setting. The root of the species tree was  
194 clock calibrated using a prior with a normal distribution defined by a mean ( $\mu$ ) of  
195 4.76 Ma and a standard deviation ( $\sigma$ ) of 1.2 Ma. The age and error range correspond

196 to those estimated for the crown node of the South American *Oreobolus* clade from a  
197 dated phylogeny of the Schoeneae tribe using one fossil and one secondary  
198 calibration (Gómez-Gutiérrez, 2016). A normal distribution was used on the root  
199 because it is the most suitable for secondary calibrations (Ho and Phillips 2009). This  
200 type of distribution allocates most of the probability density around the mean and  
201 allows for symmetrical decrease towards the tails accounting for age error (Ho and  
202 Phillips 2009). All other priors were left at their default settings.

203 Four independent MCMC runs of 250 million generations each were performed,  
204 sampling every 25000 generations. Runs were combined and 75% of the samples  
205 were discarded as burn-in. Adequate mixing and convergence were assessed using  
206 Tracer v1.6.0 (Rambaut et al. 2013). A maximum clade credibility tree (MCC) from  
207 the combined tree sets was annotated with common ancestor heights, 95% HPD node  
208 ages and posterior probability values (PP) on TreeAnnotator v2.1.2 (Rambaut and  
209 Drummond 2015).

#### 210 Haplotype definition and networks

211 Haplotypes were identified independently for the nuclear ribosomal region (ITS) and  
212 the concatenated plastid regions (*trnL-F*, *trnH-psbA* and *rpl32-trnL*) in Microsoft  
213 Excel (Microsoft Corporation, Washington DC, USA) using the Chloroplast PCR-  
214 RFLP Excel macro (French 2003). For ITS, only samples successfully sequenced for  
215 the whole region were included (Supp. Table 2). Likewise, for the concatenated  
216 plastid regions, only samples successfully sequenced for all three regions were  
217 considered (Supp. Table 2). Informative insertion/deletion events (indels) were  
218 included in the analysis and coded as absent (0) or present (1) following the simple

1  
2  
3  
4  
5  
6  
7  
8  
9  
10  
11  
12  
13  
14  
15  
16  
17  
18  
19  
20  
21  
22  
23  
24  
25  
26  
27  
28  
29  
30  
31  
32  
33  
34  
35  
36  
37  
38  
39  
40  
41  
42  
43  
44  
45  
46  
47  
48  
49  
50  
51  
52  
53  
54  
55  
56  
57  
58  
59  
60  
61  
62  
63  
64  
65

219 indel coding method of Simmons and Ochotenera (2000). Poly-T and poly-A length  
220 polymorphisms, di-nucleotide repeats and ambiguously aligned regions were  
221 excluded from subsequent analyses for all regions. Haplotype connection lengths  
222 were calculated using Arlequin ver3.5 (Excoffier and Lischer 2010) and a minimum-  
223 spanning tree was produced in Hapstar v0.5 (Teacher and Griffiths 2011).

224 NeighborNet networks – NN (Bryant and Moulton 2004) were also constructed for  
225 both nuclear and concatenated plastid haplotypes using Splitstree 4 (Huson and  
226 Bryant 2006). This method allows representation of conflicting signals in the data,  
227 which might be due to incomplete lineage sorting or reticulate evolution (Bryant and  
228 Moulton 2004; Huson and Bryant 2006). In the resulting network, conflicts are  
229 represented by parallel edges connecting taxa. The NN networks used uncorrected-p  
230 distances, which calculate the number of changes between each pair of haplotypes.

### 231 Genetic diversity and structure

232 Sampling localities were combined into clusters to increase the likelihood of  
233 detecting phylogeographic signal (Fig. 1, Supp. Table 1). Clusters were defined  
234 regardless of species classification, an approach justified by Gómez-Gutiérrez (2016;  
235 see also results below) who showed poor phylogenetic resolution amongst the South  
236 American species of *Oreobolus*. Fourteen clusters (A – N) were defined according to  
237 geographic distance and ensuring the absence of any significant geographic barrier  
238 between sampling localities within each cluster such as deep inter-Andean valleys.

239 Haplotype (h) and nucleotide ( $\pi$ ) diversities were calculated independently for each  
240 cluster and each species in Arlequin ver3.5 (Excoffier and Lischer 2010).

241 Additionally, haplotype richness (hr) was estimated for each species using  
242 HIERFSTAT (Goudet 2005) in R version 3.2.3 (R Core Team 2015). This package uses  
243 a rarefaction procedure set to 100 runs to correct for bias due to unequal sample  
244 sizes. ITS sample size was standardised to 15 individuals while cpDNA sample size  
245 was standardised to nine. Additionally,  $F_{ST}$  values between cluster pairs and species  
246 pairs were calculated independently for ITS and the concatenated plastid regions  
247 using Arlequin ver3.5 (Excoffier and Lischer 2010). NN networks for both nuclear  
248 and concatenated plastid regions were constructed from the calculated  $F_{ST}$  values.  
249 For the cluster pairs, clusters A, K and N were excluded from the analysis due to  
250 their low sample sizes ( $N \leq 2$ ). In the case of the species pairs, calculations were first  
251 undertaken considering *O. obtusangulus* as one species and then with the northern  
252 and southern populations considered as two different species.

253 To analyse the geographical structure of genetic variation, a spatial analysis of  
254 molecular variance (SAMOVA) was performed independently for the nuclear and  
255 concatenated plastid datasets (Dupanloup et al. 2002). SAMOVA identifies groups of  
256 populations/clusters that are geographically homogeneous as well as maximising  
257 genetic differentiation amongst them (Dupanloup et al. 2002). One hundred  
258 annealing simulations were undertaken for each possible number of groups (ITS,  $K =$   
259  $2 - 13$ ; cpDNA,  $K = 2 - 12$ ). The minimum number of groups ( $K$ ) was chosen that  
260 maximised the genetic differentiation amongst them ( $F_{CT}$ ). Subsequently, haplotype  
261 (h) and nucleotide ( $\pi$ ) diversities were calculated for the resulting SAMOVA groups  
262 in Arlequin ver3.5 (Excoffier and Lischer 2010). Likewise, haplotype richness (hr)  
263 was estimated for each group using HIERFSTAT (Goudet 2005) in R version 3.2.3 (R  
264 Core Team 2015). Similarly, to test if the phylogeographic structure had a

265 phylogenetic component, two measures of genetic differentiation amongst clusters  
266 were estimated using PERMUTCPSSR 2.0 (Pons and Petit 1996; Burban et al. 1999).  
267 A distance matrix was calculated based on the number of mutational steps between  
268 haplotypes ( $N_{ST}$ ) and on haplotype frequencies ( $G_{ST}$ ). Ten thousand permutations  
269 were performed to assess if  $N_{ST}$  was significantly higher than  $G_{ST}$ .

270 Additionally, variation in genetic structure was further examined for 1) all species, 2)  
271 all clusters, 3) northern Andes clusters only, 4) clusters grouped by region (northern  
272 Andes, southern Andes) and 5) SAMOVA groups using an analysis of molecular  
273 variance (AMOVA) in Arlequin ver3.5 (Excoffier and Lischer 2010).

## 274 RESULTS

### 275 Species phylogeny and timing of diversification

276 The MCC tree for the combined tree sets (Fig. 2) shows *O. cleefii*, *O. ecuadorensis*,  
277 *O. goeppingeri* and *O. venezuelensis* are recovered as monophyletic. The results  
278 support the genetic differentiation between *O. obtusangulus* from the northern Andes  
279 region (NA; Fig. 2) and *O. obtusangulus* from the southern Andes region (SA; Fig.  
280 2). *Oreobolus obtusangulus* (SA) is sister to all remaining species. In the northern  
281 Andean clade (NAC; PP=100%), *O. ecuadorensis*, *O. cleefii* and *O. obtusangulus*  
282 (NA) form a clade (PP=75%) sister to another clade composed of *O. goeppingeri* and  
283 *O. venezuelensis* (PP=71%). *Oreobolus cleefii* and *O. obtusangulus* (NA) are  
284 recovered as sister species (PP=87%). South American *Oreobolus* diverged c. 4.39  
285 Ma (95% HPD [1.96 – 6.97] Ma) during the Pliocene (Fig. 2). Subsequently, the

286 NAC diversified into five species c. 0.44 Ma (95% HPD 0.11 – 0.81] Ma) during the  
287 Pleistocene (Fig. 2).

## 288 Haplotype definition and networks

### 289 *Nuclear ribosomal DNA*

290 A total of 197 individuals from 14 clusters (A – N) were scored for ITS haplotypes,  
291 including individuals for all five species across their entire distribution range (Supp.  
292 Table 3). After exclusion of poly-T and poly-A length polymorphisms, di-nucleotide  
293 repeats and ambiguously aligned regions, 523 bp of aligned sequences remained.  
294 Thirty-nine polymorphic sites comprising 38 nucleotide substitutions and one indel  
295 defined thirty haplotypes. Of these, 22 (73.3%) were species-specific while eight  
296 (26.7%) were shared among species (Fig. 3, Supp. Table 4 and Supp. Fig. 1). There  
297 was no clear clustering according to current taxonomy evident in either the  
298 NeighborNet network (NN) (Fig. 3) or the minimum-spanning tree (MST) (Supp.  
299 Fig. 1), for example *O. obtusangulus* is not resolved in one group.

300 At a continental scale, haplotypes were geographically restricted with no shared  
301 haplotypes between the NA region and the SA (Fig. 3, Supp. Table 4 and Supp. Fig.  
302 1). This geographic structure was evident in both the minimum-spanning tree (Supp.  
303 Fig. 1) and the NN network (Fig. 3). Within the NA sampling localities, patterns  
304 were more complicated. There are eight shared haplotypes evident in the MST  
305 (Supp. Fig. 1) and many edges in the NN Network (Fig. 3). Of the eight shared  
306 haplotypes, seven occur in *O. obtusangulus*. Furthermore Hn9, a haplotype shared  
307 between *O. goeppingeri* and *O. obtusangulus*, is located in the middle of the MST  
308 connecting the SA and NA haplotypes (Supp. Fig. 1). When not considering shared

309 haplotypes, Hn12 and Hn14 found in *O. goeppingeri* are closer to those found in  
310 other species than they are to other haplotypes of the same species as are Hn28 and  
311 Hn30 in *O. venezuelensis*.

### 312 *Plastid DNA*

313 A total of 118 individuals from 13 clusters (B – N) were successfully sequenced for  
314 all three plastid markers (*trnL-F*, *trnH-psbA* and *rpl32-trnL*), including individuals  
315 from all five species across most of their distribution range (Supp. Table 3). A  
316 concatenated matrix of 2465 bp of aligned sequences (*trnL-F*, 1040 bp; *trnH-psbA*,  
317 676 bp; *rpl32-trnL*, 749 bp) resulted after the exclusion of poly-T and poly-A length  
318 polymorphisms, di-nucleotide repeats and ambiguously aligned regions. Forty  
319 haplotypes were identified based on 141 polymorphic sites (*trnL-F*, 53; *trnH-psbA*,  
320 14; *rpl32-trnL*, 74) including 112 nucleotide substitutions and 28 indels. Thirty-four  
321 haplotypes (85%) were species-specific while six (15%) were shared among species  
322 (Fig. 4, Supp. Table 5 and Supp. Fig. 2). When only considering species-specific  
323 haplotypes, both the MST and NN network showed some degree of clustering  
324 according to taxonomy for three of the species, namely *O. ecuadorensis*, *O.*  
325 *goeppingeri* and *O. venezuelensis* (Fig. 4 and Supp. Fig. 2).

326 As for ITS, there were no shared haplotypes between the NA and the SA regions  
327 (Fig. 4, Supp. Table 5 and Supp. Fig. 2). This geographic structure was evident in  
328 both the MST and the NN network (Fig. 4 and Supp. Fig. 2). There was low support  
329 for groupings in the cpDNA network in the relationships amongst NA groups  
330 compounded by the large number of possible unsampled haplotypes. The results of



331 the cpDNA analysis were similar to those of ITS in showing a large number of edges  
332 and of shared haplotypes.

### 333 Genetic diversity and structure

#### 334 *Species genetic structure*

335 Molecular diversity indices for ITS and cpDNA for the five *Oreobolus* species,  
336 including the two *O. obtusangulus* groups (NA and SA), are shown in Table 1.

337 Haplotype and nucleotide diversity was lowest in *O. ecuadorensis* and highest in *O.*  
338 *obtusangulus* (Table 1). Similarly, haplotypic richness was lowest in *O. ecuadorensis*  
339 and highest in *O. obtusangulus*. However, the high values in *O. obtusangulus* were  
340 reduced when considering SA and NA populations of *O. obtusangulus* as separate  
341 species (see Table 1).

342 Pairwise  $F_{ST}$  values between all species pairs were significant for ITS and cpDNA  
343 (ITS:  $p < 0.001$ ; cpDNA:  $p < 0.05$ ), with the exception of *O. cleefii* and *O.*

344 *obtusangulus* (NA) for cpDNA ( $F_{ST} = -0.020$ ) (Table 2, Supp. Figs 3 – 4).

345 *Oreobolus ecuadorensis* is consistently differentiated from the other species in both  
346 ITS and cpDNA (Table 2, Supp. Figs 3 – 4). The NN, based on  $F_{ST}$  values showed

347 that when considering *O. obtusangulus* as one species, it is reconstructed in the

348 middle of the network and its placement is poorly resolved in both ITS and cpDNA

349 NN networks (Supp. Figs 3a – 4a). In contrast, when considering northern and

350 southern groups separately, *O. obtusangulus* (SA) is clearly different from other

351 *Oreobolus* species, whereas *O. obtusangulus* (NA) has affinities with *O. cleefii*. The

352 conflicting signal between the latter two species (i.e., multiple parallel edges) is

353 evident in both cpDNA and ITS NN networks (Supp. Figs 3b – 4b). *Oreobolus*

354 *goeppingeri* and *O. venezuelensis* are well differentiated in cpDNA but not in ITS  
355 where they appeared in the centre of the networks with multiple connections to the  
356 other species (Supp. Figs 3 – 4).

### 357 *Cluster genetic structure*

358 The results of the AMOVA showed that although differentiation amongst species  
359 was significant (ITS,  $F_{ST} = 0.30$ ,  $p < 0.001$ ; cpDNA,  $F_{ST} = 0.48$ ,  $p < 0.001$ ), within  
360 species variation accounted for 70% for ITS and 52% for cpDNA (Table 3).  
361 Similarly, separation into geographic clusters only explained 43% (ITS) and 37%  
362 (cpDNA) of the variation.

363 The SAMOVA for both ITS and cpDNA indicated three groups (I – III; Supp. Table  
364 8, Supp. Figs 1 – 2) as the number of genetic clusters (K) that maximised genetic  
365 differentiation amongst groups while minimising the number of single-cluster groups  
366 (ITS,  $F_{CT} = 0.622$ ,  $p < 0.001$ ; cpDNA,  $F_{CT} = 0.426$ ,  $p < 0.001$ ). For ITS, group I  
367 included all NA clusters (A – J) while groups II (K, L, N) and III (M) included the  
368 SA ones (Supp. Table 8, Supp. Fig. 1). For cpDNA, group I included all NA clusters  
369 plus the northernmost SA cluster (K), while groups II (L, N) and III (M) included the  
370 rest (Supp. Table 8, Supp. Fig. 2). SAMOVA groups explained slightly more of the  
371 genetic structure (ITS,  $F_{CT} = 0.62$ ,  $p < 0.001$ ; cpDNA,  $F_{CT} = 0.43$ ,  $p < 0.001$ ) than the  
372 NA versus SA continental divide (ITS,  $F_{CT} = 0.60$ ,  $p < 0.001$ ; cpDNA,  $F_{CT} = 0.36$ ,  $p$   
373  $< 0.001$ ) (Table 3). Molecular diversity indices calculated for the SAMOVA groups  
374 are presented in Table 4. Significant phylogeographic structure was indicated by the  
375 significantly higher values of  $N_{ST}$  (ITS,  $N_{ST} = 0.605$ ; cpDNA,  $N_{ST} = 0.406$ )  
376 compared to  $G_{ST}$  (ITS,  $G_{ST} = 0.262$ ; cpDNA,  $G_{ST} = 0.156$ ;  $p < 0.01$ ).

377 DISCUSSION

378 Timing of diversification

379 The dated species tree presented here (Fig. 2) indicates younger diversification dates  
380 than those presented by Chacón et al. (2006), which is expected because divergence  
381 dates estimated from a species tree will generally be younger than those estimated  
382 from a gene tree (Drummond and Bouckaert 2015). Our species phylogeny indicates  
383 that the most recent common ancestor of the South American *Oreobolus* diverged  
384 4.39 Ma (95% HPD [1.96 – 6.97] Ma) during the late Miocene – early Pliocene.  
385 Subsequently, the northern Andean clade (NAC) appears to have diversified from  
386 0.44 Ma (95% HPD [0.11 – 0.81] Ma). This indicates that the expansion and  
387 contraction of Páramo islands during the glacial cycles of the Quaternary may have  
388 played a role in diversification in the northern Andes (see last section of the  
389 discussion) (van der Hammen 1974; Simpson 1975; van der Hammen and Cleef  
390 1986; Hooghiemstra and van der Hammen 2004).

391 Genetic diversity and structure

392 Our results reveal a complex evolutionary history for the five South American  
393 species of *Oreobolus*. Species relationships were difficult to estimate, indicating  
394 either interspecific gene flow and/or incomplete lineage sorting (Naciri and Linder  
395 2015). Haplotype and nucleotide diversity were high for both ITS and cpDNA for all  
396 species except *O. ecuadorensis* (Table 1). Additionally, shared haplotypes were  
397 observed in both ITS (27%) and cpDNA (15%). This intricate history is also evident

398 in the MST and NN networks for both ITS and cpDNA (Figs. 3 – 4 and Supp. Figs. 1  
399 – 2).

400 The high degree of complexity observed amongst these species contrasts with the  
401 morphological characters that distinguish them. Inconsistencies between  
402 morphological characteristics and genetic patterns can arise due to high levels of  
403 plasticity of morphological characters or parallel adaptations to local conditions  
404 resulting in the same morphology, which might be the case for *O. obtusangulus*. The  
405 data presented here indicate that the two subspecies of *O. obtusangulus* represent  
406 morphologically cryptic species. Britton et al. (2014) have described another  
407 example of cryptic speciation within the Schoeneae in the South African species  
408 *Tetraria triangularis*. These authors found at least three intraspecific lineages that  
409 qualified as cryptic species based on their genetic distinctiveness and subtle  
410 morphological differentiation. Furthermore, cryptic lineages have also been found in  
411 otherwise morphologically indistinguishable taxa within the Páramo genus *Loricaria*  
412 (Asteraceae) (Kolář et al. 2016).

413 Nonetheless, convergent morphological evolution does not appear to satisfactorily  
414 account for the genetic patterns observed in many South American species of  
415 *Oreobolus*, which may result from incomplete lineage sorting (ILS) and/or  
416 hybridization. Given the recent Pliocene diversification of both the northern and  
417 southern Andean clades of *Oreobolus* (Fig. 2), lineage sorting may not have been  
418 fully completed. Previous studies have indicated ILS in recently diverged groups,  
419 particularly when effective population sizes are large (Maddison and Knowles 2006;  
420 Jakob and Blattner 2006; Degnan and Rosenberg 2009; Cutter 2013). Furthermore,  
421 under a scenario of ILS, it is expected that different genes would have different

1  
2  
3  
4  
5  
6  
7  
8  
9  
10  
11  
12  
13  
14  
15  
16  
17  
18  
19  
20  
21  
22  
23  
24  
25  
26  
27  
28  
29  
30  
31  
32  
33  
34  
35  
36  
37  
38  
39  
40  
41  
42  
43  
44  
45  
46  
47  
48  
49  
50  
51  
52  
53  
54  
55  
56  
57  
58  
59  
60  
61  
62  
63  
64  
65

422 coalescence times. Haploid plastid genes have a lower effective population size than  
423 nuclear genes and thus would coalesce faster (Schaal and Olsen 2000; Naciri and  
424 Linder 2015). Faster coalescence would be translated into an increased  
425 correspondence between the genetic relationships recovered with plastid genes and  
426 currently recognised taxonomic species. Our results support this scenario because  
427 cpDNA better differentiates taxonomic species than ITS for *O. ecuadorensis*, *O.*  
428 *goeppingeri* and *O. venezuelensis* (Figs. 3 – 4 and Supp. Figs. 1 – 2).

429 However, species relationships may be obscured by ongoing gene flow as patterns of  
430 ILS are difficult to disentangle from those of historic hybridization. Two species  
431 pairs, *Oreobolus cleefii* and *O. obtusangulus* (NA), and *O. goeppingeri* and *O.*  
432 *venezuelensis*, show patterns indicative of ILS and/or hybridization. Firstly,  
433 *Oreobolus cleefii* and *O. obtusangulus* (NA) show contrasting patterns between  
434 nuclear (ITS) and cpDNA haplotypes (Figs. 3 – 4 and Supp. Figs. 1 – 2) possibly due  
435 to chloroplast capture and simultaneous nuclear introgression (Abbott et al. 2013).  
436 These closely related species naturally occur in sympatry in all of the sampled  
437 localities (Fig. 1) and show an overlap in morphological characters (Seberg 1988). In  
438 fact, morphological similarities previously lead Seberg (1988) to suggest that *O.*  
439 *cleefii* should be reduced to synonymy under *O. obtusangulus* subsp. *unispicus*, the  
440 northern Andean subspecies of *O. obtusangulus*. Secondly, the two most widespread  
441 species in the Páramo, *O. goeppingeri* and *O. venezuelensis*, also naturally occur in  
442 sympatry in all sampled localities (Fig. 1). These species also show complicated  
443 genetic patterns, combining high levels of diversity with shared haplotypes (Figs. 3  
444 and 4) and conflicting phylogenetic relationships (Supp. Figs. 3 – 4 with other  
445 northern Andean species). A possible explanation is that the widespread nature of

1  
2  
3  
4  
5  
6  
7  
8  
9  
10  
11  
12  
13  
14  
15  
16  
17  
18  
19  
20  
21  
22  
23  
24  
25  
26  
27  
28  
29  
30  
31  
32  
33  
34  
35  
36  
37  
38  
39  
40  
41  
42  
43  
44  
45  
46  
47  
48  
49  
50  
51  
52  
53  
54  
55  
56  
57  
58  
59  
60  
61  
62  
63  
64  
65

446 these species provided greater opportunities for intra, and interspecific mixing  
447 compared with more range-restricted species, which exhibit a similar pattern of  
448 haplotype sharing, albeit on a smaller scale (Supp. Figs. 1 – 2).

449 Current gene flow would be expected to result in F1 hybrids that would exhibit  
450 heterozygosity in ITS, but this was not observed in any *Oreobolus* species, although  
451 such heterozygosity may no longer be evident in older hybrids. While the presence of  
452 later generations of hybrids or backcrosses cannot be excluded, the lack of  
453 heterozygosity in ITS and the presence of shared haplotypes recovered in multiple  
454 pairs of individuals from all species is more suggestive of a stochastic process likely  
455 related to lineage sorting. Therefore, although gene flow cannot be ruled out and may  
456 have a role in some situations (e.g. *Oreobolus cleefii* and *O. obtusangulus* see  
457 below), we suggest incomplete lineage sorting in a recently diversified group is also  
458 part of the explanation for the complex patterns observed in the South American  
459 species of *Oreobolus*. A recent phylogeographic study of the Australian alpine *Poa*  
460 (Poaceae) describes a similar pattern of problematic recovery of species relationships  
461 associated with a putatively young ecosystem and a Pleistocene radiation following  
462 long-distance dispersal to Australia (Griffin and Hoffmann 2014). This study also  
463 favoured ILS rather than ongoing gene flow as the likely process behind the  
464 observed pattern based on the widespread genetic similarity and recent divergence  
465 times.

466 The results of the AMOVAs revealed that neither clustering into currently defined  
467 taxonomic species (Mora-Osejo 1987; Seberg 1988) nor into our pre-defined  
468 geographic clusters (Fig. 1, Supp. Table 1) described the distribution of genetic  
469 diversity, only explaining 30% (ITS)/48% (cpDNA) and 43% (ITS)/37% (cpDNA),

1  
2  
3  
4  
5  
6  
7  
8  
9  
10  
11  
12  
13  
14  
15  
16  
17  
18  
19  
20  
21  
22  
23  
24  
25  
26  
27  
28  
29  
30  
31  
32  
33  
34  
35  
36  
37  
38  
39  
40  
41  
42  
43  
44  
45  
46  
47  
48  
49  
50  
51  
52  
53  
54  
55  
56  
57  
58  
59  
60  
61  
62  
63  
64  
65

470 respectively (Table 3). Rather, the SAMOVA suggested that an *a posteriori*  
471 geographic arrangement better explained genetic diversity (62% for ITS and 43% for  
472 cpDNA, Table 3). Thus, the observed patterns of genetic diversity are likely to be the  
473 result of complex interactions between some species over various geographic  
474 distances.

475 At a continental scale there is evidence of geographic structure in *Oreobolus* species,  
476 (Figs. 1 – 2, Supp. Figs. 1 – 2), suggested by a higher value of  $N_{ST}$  compared to  $G_{ST}$   
477 ( $p < 0.01$ ), indicating that haplotypes in the same cluster are on average more closely  
478 related than distinct haplotypes from different clusters. The clearest geographic break  
479 apparent in *Oreobolus* is between the northern Andes (NA) and southern Andes  
480 (SA). This pattern is evident in both chloroplast and nuclear regions, although the  
481 pattern is much stronger in ITS (Figs. 1 – 2, Supp. Figs. 1 – 2). The arid central  
482 Andes are likely to impose a barrier to dispersal and gene flow, but the position of  
483 the north-south break is unclear. SAMOVA groups clearly identify the NA/SA  
484 disjunction in ITS but not in the plastid region where cluster K is grouped with the  
485 northern Andean clusters (Supp. Table 8, Supp. Figs. 1 – 2). The latter is also evident  
486 in the cpDNA NN where the distance between haplotypes is shorter than in the NN  
487 for ITS (Figs. 1 – 2). The incongruence between ITS and plastid regions may suggest  
488 mixing between the SAC and NAC in cluster K, resulting from long distance  
489 dispersal events. Cluster K is separated from both NA clusters and other SA clusters  
490 by a substantial distance and possesses unique haplotypes at both ITS and plastid  
491 regions (Supp. Tables 4 – 5).

492 Additional structure is evident at regional scales within the NAC and appears to be  
493 associated with putative geographic barriers to gene flow. Pairwise  $F_{ST}$  values

1  
2  
3  
4  
5  
6  
7  
8  
9  
10  
11  
12  
13  
14  
15  
16  
17  
18  
19  
20  
21  
22  
23  
24  
25  
26  
27  
28  
29  
30  
31  
32  
33  
34  
35  
36  
37  
38  
39  
40  
41  
42  
43  
44  
45  
46  
47  
48  
49  
50  
51  
52  
53  
54  
55  
56  
57  
58  
59  
60  
61  
62  
63  
64  
65

494 calculated for ITS showed that clusters B and J were significantly differentiated from  
495 all other sites, regardless of the geographic distances (Fig. 5, Supp. Table 7). These  
496 two clusters are separated from all other NA clusters by inter-Andean valleys of  
497 seasonally dry tropical forest. Cluster B is isolated from the rest by the dry  
498 Chicamocha Canyon while cluster J is separated from the other NA clusters by the  
499 Marañón Valley (Fig. 1). Särkinen et al. (2012) suggested that biome heterogeneity  
500 across the Andes represented a strong barrier to dispersal within island-like  
501 ecosystems. This is particularly relevant when deep valleys segment the mountain  
502 ranges, as is the case here. In addition, for *O. venezuelensis*, clusters H and I have  
503 ITS haplotypes distinct from others in the species, namely Hn28 and Hn30 (Fig. 1,  
504 Supp. Fig. 1). These haplotypes are distributed in the southernmost part of these  
505 species' distribution range and their differentiation from species-specific haplotypes  
506 distributed in the northernmost areas (Hn26, Hn27 and Hn28) further supports the  
507 observed phylogeographic structure and possible pattern of isolation by distance.

#### 508 Genetic patterns in the light of Quaternary glacial-interglacial cycles.

509 Our dated tree (Fig. 2) is consistent with Quaternary diversification in the NAC, and  
510 high levels of molecular diversity for both nuclear and plastid regions, as well as the  
511 high number of unsampled cpDNA haplotypes in our dataset, are concordant with a  
512 scenario of expansion and contraction of Páramo islands during the glacial cycles of  
513 the Quaternary (Table 4, Supp. Table 8 and Supp. Fig. 2). SAMOVA analysis failed  
514 to identify any clear groupings within the NAC (Supp. Table 8, Supp. Figs. 1 – 2)  
515 and variation amongst NA clusters was moderate and mostly explained by within  
516 cluster variation (ITS, 86%; cpDNA, 79%; Table 3). Vicariance events would allow



1  
2  
3  
4  
5  
6  
7  
8  
9  
10  
11  
12  
13  
14  
15  
16  
17  
18  
19  
20  
21  
22  
23  
24  
25  
26  
27  
28  
29  
30  
31  
32  
33  
34  
35  
36  
37  
38  
39  
40  
41  
42  
43  
44  
45  
46  
47  
48  
49  
50  
51  
52  
53  
54  
55  
56  
57  
58  
59  
60  
61  
62  
63  
64  
65

517 for differentiation of populations and diversification, through selection and drift. If  
518 reproductive isolation is incomplete, subsequent expansion events may have allowed  
519 gene flow amongst nearby populations and potentially even amongst species.  
520 Repeated vicariance and contact, which would be expected from Quaternary glacial  
521 cycles, would generate complex genetic patterns, with species sharing haplotypes.  
522 Such patterns are evident in *Oreobolus*, with a few widespread haplotypes amongst  
523 species apparently giving rise to geographically restricted haplotypes (Supp. Figs. 1  
524 – 2). Similar patterns have been reported for the afro-alpine populations of *Arabis*  
525 *alpina* where several cycles of range contraction and expansion caused by the glacial  
526 cycles of the Quaternary may have shaped intra-specific distribution of genetic  
527 diversity (Assefa et al. 2007). In the same way, cluster M in the SA region is a  
528 divergent genetic group for both ITS and cpDNA in SAMOVA analyses (Supp. Figs.  
529 1 – 2). Molecular diversity indices for this cluster showed low haplotype diversity  
530 and high nucleotide diversity in ITS, and high haplotype diversity and low nucleotide  
531 diversity in cpDNA (Supp. Table 8). A possible explanation for this pattern might be  
532 that these populations underwent a bottleneck during isolation resulting in a low  
533 number of divergent haplotypes. During the glacial cycles of the Quaternary ice  
534 sheets covered extensive areas and generated massive fragmentation and restriction  
535 in the distribution of southern Andean plants producing pockets of refugial  
536 populations (e.g. Markgraf et al. 1995). Although a scenario of Pleistocene refugia  
537 has already been proposed for other southern Andean plants (e.g. Tremetsberger et  
538 al. 2009) further work would be required to assess the potential for refugial  
539 populations in *O. obtusangulus* (SA).

1  
2  
3  
4  
5  
6  
7  
8  
9  
10  
11  
12  
13  
14  
15  
16  
17  
18  
19  
20  
21  
22  
23  
24  
25  
26  
27  
28  
29  
30  
31  
32  
33  
34  
35  
36  
37  
38  
39  
40  
41  
42  
43  
44  
45  
46  
47  
48  
49  
50  
51  
52  
53  
54  
55  
56  
57  
58  
59  
60  
61  
62  
63  
64  
65

540 Glacial cycles may have also had an impact at the inter-specific level. *Oreobolus*  
541 *ecuadorensis* has the lowest molecular diversity indices for both ITS and cpDNA  
542 (Table 1) and is one of the most geographically restricted species, found only in  
543 Ecuador and northern Peru (Fig. 1). Such patterns may arise through a severe  
544 bottleneck followed by a population expansion likely imposed by the glacial cycles  
545 of the Quaternary (Templeton 1998; Hewitt 2004). Ecuador and Peru have the  
546 highest percentage of permanent snow and therefore interglacial periods may have  
547 greatly reduced the size of the populations of *O. ecuadorensis*, reducing its genetic  
548 diversity. Following the Last Glacial Maximum (LGM), population expansion may  
549 have occurred with new mutations likely to accumulate as the species occupied new  
550 areas. New haplotypes were thereby produced, diverging from the founder  
551 population by only a few nucleotides. At the same time, the strong impact of  
552 interglacial periods is evident in the clear differentiation of *O. ecuadorensis* from all  
553 other species (Table 2, Supp. Figs. 3 – 4).

554 There was no clear evidence of ongoing hybridization but historic hybridization  
555 between sympatric sister species *O. cleefii* and *O. obtusangulus* (NA) may have been  
556 facilitated by periods of isolation and divergence during the glacial cycles of the  
557 Quaternary. Secondary contact zones can form from long-distance dispersal events,  
558 leading to interspecific hybridization, such as that proposed by Gizaw et al. (2016)  
559 for two co-occurring sister species of *Carex* from a similar tropical alpine ecosystem  
560 in East Africa. We suggest a similar scenario for *O. cleefii* and *O. obtusangulus*  
561 (NA), with renewed contact occurring following isolation during interglacial periods  
562 in the Quaternary (van der Hammen 1974).

563 CONCLUSION

1  
2  
3 564 This is one of a few studies to investigate genetic relationships both within and  
4  
5 565 between species in a recently diverged Páramo genus and hence it provides a  
6  
7 566 significant contribution to the understanding of the historical assembly of the Páramo  
8  
9  
10 567 flora. The results presented here are consistent with a role for contraction and  
11  
12 568 expansion of Páramo islands during glacial cycles in the diversification of *Oreobolus*  
13  
14 569 species. ILS appears to have played a role in the complex genetic patterns observed  
15  
16 570 amongst these recently diverged *Oreobolus* species. ILS rather than recent  
17  
18 571 hybridization is suggested by the lack of heterozygosity in ITS, but a role for  
19  
20 572 historical hybridization cannot be discounted, particularly in several situations where  
21  
22 573 the species are sympatric. Additional work incorporating more extensive sampling of  
23  
24 574 individuals and assessing additional genetic data will be required to more accurately  
25  
26 575 estimate patterns of historical demography of *Oreobolus*, which could bring further  
27  
28 576 insight into the population dynamics of Páramo plants.  
29  
30  
31  
32  
33  
34  
35  
36  
37  
38  
39  
40  
41  
42  
43  
44  
45  
46  
47  
48  
49  
50  
51  
52  
53  
54  
55  
56  
57  
58  
59  
60  
61  
62  
63  
64  
65

577

1 578 CONFLICT OF INTEREST  
2  
3  
4

5 579 The authors declare that they have no conflict of interest.  
6  
7  
8  
9

10 580 DECLARATION OF AUTHORSHIP  
11  
12  
13  
14

15 581 MCGG and JER devised the project. LEN assisted with data analyses. MCGG  
16  
17 582 drafted the text, with substantial contributions by JER, RTP and LEN. All authors  
18  
19 583 contributed to final editing.  
20  
21  
22  
23  
24

25 REFERENCES  
26  
27  
28  
29

- 30 584 Abbott R, Albach D, Ansell S, et al (2013) Hybridization and speciation. *J Evol Biol*  
31 585 26:229–246. doi: 10.1111/j.1420-9101.2012.02599.x  
32  
33 586 Arnold ML (1997) Natural hybridization and evolution. Oxford University Press,  
34 587 New York  
35  
36  
37 588 Assefa A, Ehrich D, Taberlet P, et al (2007) Pleistocene colonization of afro-alpine  
38 589 “sky islands” by the arctic-alpine *Arabis alpina*. *Heredity* 99:133–142. doi:  
39 590 10.1038/sj.hdy.6800974  
40  
41  
42 591 Bouckaert R, Drummond AJ (2017) bModelTest: Bayesian phylogenetic site model  
43 592 averaging and model comparison. *BMC Evolutionary Biology* 17:1–11. doi:  
44 593 10.1186/s12862-017-0890-6  
45  
46 594 Bouckaert R, Heled J, Kühnert D, et al (2014) BEAST 2: A Software Platform for  
47 595 Bayesian Evolutionary Analysis. *PLoS Comput Biol* 10:e1003537–6. doi:  
48 596 10.1371/journal.pcbi.1003537  
49  
50  
51 597 Britton MN, Hedderson TA, Verboom GA (2014) Topography as a driver of cryptic  
52 598 speciation in the high-elevation cape sedge *Tetraria triangularis* (Boeck.) C. B.  
53 599 Clarke (Cyperaceae: Schoeneae). *Molecular Phylogenetics and Evolution* 77:96–  
54 600 109. doi: 10.1016/j.ympev.2014.03.024  
55  
56  
57  
58  
59  
60  
61  
62  
63  
64  
65

- 1  
2  
3  
4  
5  
6  
7  
8  
9  
10  
11  
12  
13  
14  
15  
16  
17  
18  
19  
20  
21  
22  
23  
24  
25  
26  
27  
28  
29  
30  
31  
32  
33  
34  
35  
36  
37  
38  
39  
40  
41  
42  
43  
44  
45  
46  
47  
48  
49  
50  
51  
52  
53  
54  
55  
56  
57  
58  
59  
60  
61  
62  
63  
64  
65
- 601 Bryant D, Moulton V (2004) Neighbor-Net: An Agglomerative Method for the  
602 Construction of Phylogenetic Networks. *Molecular Biology and Evolution*  
603 21:255–265. doi: 10.1093/molbev/msh018
- 604 Burban C, Petit R, Carcreff E, Jactel H (1999) Rangewide variation of the maritime  
605 pine bast scale *Matsucoccus feytaudi* Duc. (Homoptera: Matsucoccidae) in  
606 relation to the genetic structure of its host. *Mol Ecol* 8:1593–1602.
- 607 Buytaert W, Cuesta-Camacho F, Tobón C (2010) Potential impacts of climate  
608 change on the environmental services of humid tropical alpine regions. *Global*  
609 *Ecology and Biogeography* 20:19–33. doi: 10.1111/j.1466-8238.2010.00585.x
- 610 Chacón J, Madriñán S, Chase MW, Bruhl JJ (2006) Molecular phylogenetics of  
611 *Oreobolus* (Cyperaceae) and the origin and diversification of the American  
612 species. *Taxon* 55:359–366.
- 613 Cutter AD (2013) Integrating phylogenetics, phylogeography and population  
614 genetics through genomes and evolutionary theory. *Molecular Phylogenetics and*  
615 *Evolution* 69:1172–1185. doi: 10.1016/j.ympev.2013.06.006
- 616 Degnan JH, Rosenberg NA (2009) Gene tree discordance, phylogenetic inference  
617 and the multispecies coalescent. *Trends in Ecology & Evolution* 24:332–340.  
618 doi: 10.1016/j.tree.2009.01.009
- 619 Doyle J, Doyle JL (1990) Isolation of plant DNA from fresh tissue. *Focus* 12:13–15.
- 620 Drummond AJ, Bouckaert RR (2015) *Bayesian Evolutionary Analysis with BEAST*,  
621 First. Cambridge University Press, Cambridge
- 622 Dupanloup I, Schneider S, Excoffier L (2002) A simulated annealing approach to  
623 define the genetic structure of populations. *Mol Ecol* 11:2571–2581.
- 624 Excoffier L, Lischer HEL (2010) Arlequin suite ver 3.5: a new series of programs to  
625 perform population genetics analyses under Linux and Windows. *Molecular*  
626 *Ecology Resources* 10:564–567. doi: 10.1111/j.1755-0998.2010.02847.x
- 627 French GC (2003) *Conservation genetics of British Euphrasia L.* University of  
628 Edinburgh and Royal Botanic Garden Edinburgh, Edinburgh
- 629 Gizaw A, Kebede M, Nemomissa S, et al (2013) Phylogeography of the heathers  
630 *Erica arborea* and *E. trimera* in the afro-alpine “sky islands” inferred from  
631 AFLPs and plastid DNA sequences. *Flora* 208:453–463. doi:  
632 10.1016/j.flora.2013.07.007
- 633 Gizaw A, Wondimu T, Mugizi TF, et al (2016) Vicariance, dispersal, and  
634 hybridization in a naturally fragmented system: the afro-alpine endemics *Carex*  
635 *monostachya* and *C. runssoroensis* (Cyperaceae). *Alpine Botany* 126:59–71. doi:  
636 10.1007/s00035-015-0162-2
- 637 Goudet J (2005) Hierfstat, a package for R to compute and test hierarchical F-

- 638 statistics. *Molecular Ecology Notes* 5:184–186. doi: 10.1111/j.1471-8278  
639 .2004.00828.x
- 640 Gómez-Gutiérrez MC (2016) Evolution in the high-altitude Páramo ecosystem. The  
641 University of Edinburgh PhD thesis.
- 642 Graham A (2009) The Andes: a geological overview from a biological perspective.  
643 *Annals of the Missouri Botanical Garden* 96:371–385. doi: 10.3417/2007146
- 644 Griffin PC, Hoffmann AA (2014) Limited genetic divergence among Australian  
645 alpine *Poa* tussock grasses coupled with regional structuring points to ongoing  
646 gene flow and taxonomic challenges. *Annals of Botany* 113:953–965. doi:  
647 10.1093/aob/mcu017
- 648 Heled J, Drummond AJ (2012) Calibrated Tree Priors for Relaxed Phylogenetics and  
649 Divergence Time Estimation. *Systematic Biology* 61:138–149. doi:  
650 10.1093/sysbio/syr087
- 651 Hewitt GM (2004) Genetic consequences of climatic oscillations in the Quaternary.  
652 *Philosophical Transactions of the Royal Society B: Biological Sciences*  
653 359:183–195. doi: 10.1098/rstb.2003.1388
- 654 Ho SYW, Phillips MJ (2009) Accounting for calibration uncertainty in phylogenetic  
655 estimation of evolutionary divergence times. *Systematic Biology* 58:367–380.  
656 doi: 10.1093/sysbio/syp035
- 657 Hooghiemstra H, van der Hammen T (2004) Quaternary Ice-Age dynamics in the  
658 Colombian Andes: developing an understanding of our legacy. *Philosophical*  
659 *Transactions of the Royal Society B: Biological Sciences* 359:173–181. doi:  
660 10.1098/rstb.2003.1420
- 661 Hooghiemstra H, Wijninga VM, Cleef AM (2006) The paleobotanical record of  
662 Colombia: implications for biogeography and biodiversity. *Annals of the*  
663 *Missouri Botanical Garden* 93:297–324. doi: 10.3417/0026-  
664 6493(2006)93[297:TPROCI]2.0.CO;2
- 665 Huson DH, Bryant D (2006) Application of phylogenetic networks in evolutionary  
666 studies. *Molecular Biology and Evolution* 23:254–267. doi:  
667 10.1093/molbev/msj030
- 668 Jakob SS, Blattner FR (2006) A chloroplast genealogy of *Hordeum* (Poaceae): long-  
669 term persisting haplotypes, incomplete lineage sorting, regional extinction, and  
670 the consequences for phylogenetic inference. *Molecular Biology and Evolution*  
671 23:1602–1612. doi: 10.1093/molbev/msl018
- 672 Kadu CAC, Konrad H, Schueler S, et al (2013) Divergent pattern of nuclear genetic  
673 diversity across the range of the Afrotropical *Prunus africana* mirrors variable  
674 climate of African highlands. *Annals of Botany* 111:47–60. doi:  
675 10.1093/aob/mcs235

- 1  
2  
3  
4  
5  
6  
7  
8  
9  
10  
11  
12  
13  
14  
15  
16  
17  
18  
19  
20  
21  
22  
23  
24  
25  
26  
27  
28  
29  
30  
31  
32  
33  
34  
35  
36  
37  
38  
39  
40  
41  
42  
43  
44  
45  
46  
47  
48  
49  
50  
51  
52  
53  
54  
55  
56  
57  
58  
59  
60  
61  
62  
63  
64  
65
- 676 Kebede M, Ehrich D, Taberlet P, et al (2007) Phylogeography and conservation  
677 genetics of a giant lobelia (*Lobelia giberroa*) in Ethiopian and Tropical East  
678 African mountains. *Mol Ecol* 16:1233–1243. doi: 10.1111/j.1365-  
679 294X.2007.03232.x
- 680 Kolář F, Dušková E, Sklenář P (2016) Niche shifts and range expansions along  
681 cordilleras drove diversification in a high-elevation endemic plant genus in the  
682 tropical Andes. *Mol Ecol* 25:4593–4610. doi: 10.1111/mec.13788
- 683 Luteyn JL (1999) Páramos: a checklist of plant diversity, geographical distribution,  
684 and botanical literature, First. The New York Botanical Garden Press, New York
- 685 Maddison WP, Knowles LL (2006) Inferring phylogeny despite incomplete lineage  
686 sorting. *Systematic Biology* 55:21–30. doi: 10.1080/10635150500354928
- 687 Maddison WP, Maddison DR (2014) Mesquite: a modular system for evolutionary  
688 analysis. Version 2.75. Available at <http://mesquiteproject.org>. –  
689 [mesquiteproject.org](http://mesquiteproject.org).
- 690 Madriñán S, Cortés AJ, Richardson JE (2013) Páramo is the world's fastest evolving  
691 and coolest biodiversity hotspot. *Frontiers in Genetics* 4:1–7. doi:  
692 10.3389/fgene.2013.00192/abstract
- 693 Markgraf V, McGlone M, Hope G (1995) Neogene paleoenvironmental and  
694 paleoclimatic change in southern temperate ecosystems—a southern perspective.  
695 *Trends in Ecology & Evolution* 10:143–147. doi: 10.1016/S0169-  
696 5347(00)89023-0
- 697 Moore DM (1967) Chromosome numbers of Falkland Islands Angiosperms. *British*  
698 *Antarctic Survey Bulletin* 14:69–82.
- 699 Mora-Osejo LE (1987) Estudios morfológicos, autoecológicos y sistemáticos en  
700 Angiospermas. Academia Colombiana de Ciencias Exactas, Físicas y Naturales,  
701 Bogotá, DE
- 702 Möller M, Cronk QCB (1997) Origin and relationships of *Saintpaulia* (Gesneriaceae)  
703 based on ribosomal DNA internal transcribed spacer (ITS) sequences. *American*  
704 *Journal of Botany* 84:956–965.
- 705 Naciri Y, Linder HP (2015) Species delimitation and relationships: The dance of the  
706 seven veils. *Taxon* 64:3–16. doi: 10.12705/641.24
- 707 Pons O, Petit RJ (1996) Measuring and testing genetic differentiation with ordered  
708 versus unordered alleles. *Genetics* 144:1237–1245.
- 709 R Core Team (2015) R: A language and environment for statistical computing. R  
710 Foundation for Statistical Computing, Vienna, Austria. Available at  
711 <https://www.R-project.org/>. <https://www.R-project.org>
- 712 Rambaut A, Drummond AJ (2015) TreeAnnotator: MCMC output analysis. Version

- 713 2.3.0. Available at <http://tree.bio.ed.ac.uk/software/beast>.  
714 <http://tree.bio.ed.ac.uk/software>
- 715 Rambaut A, Suchard MA, Xie W, Drummond AJ (2013) Tracer: MCMC trace  
716 analysis tool. Version 1.6.0. Available at <http://tree.bio.ed.ac.uk/software/tracer>.  
717 <http://tree.bio.ed.ac.uk/software>
- 718 Sang T, Crawford D, Stuessy T (1997) Chloroplast DNA phylogeny, reticulate  
719 evolution, and biogeography of *Paeonia* (Paeoniaceae). *American Journal of*  
720 *Botany* 84:1120–1136.
- 721 Särkinen T, Pennington RT, Lavin M, et al (2012) Evolutionary islands in the Andes:  
722 persistence and isolation explain high endemism in Andean dry tropical forests.  
723 *Journal of Biogeography* 39:884–900. doi: 10.1111/j.1365-2699.2011.02644.x
- 724 Schaal BA, Hayworth DA, Olsen KM, et al (1998) Phylogeographic studies in  
725 plants: problems and prospects. *Mol Ecol* 7:465–474. doi: 10.1046/j.1365-  
726 294x.1998.00318.x
- 727 Schaal BA, Olsen KM (2000) Gene genealogies and population variation in plants.  
728 *Proc Natl Acad Sci USA* 97:7024–7029.
- 729 Seberg O (1988) Taxonomy, phylogeny, and biogeography of the genus *Oreobolus*  
730 R.Br. (Cyperaceae), with comments on the biogeography of the South Pacific  
731 continents. *Botanical Journal of the Linnean Society* 96:119–195. doi:  
732 10.1111/j.1095-8339.1988.tb00632.x
- 733 Shaw J, Lickey EB, Schilling EE, Small RL (2007) Comparison of whole chloroplast  
734 genome sequences to choose noncoding regions for phylogenetic studies in  
735 Angiosperms: the tortoise and the hare III. *American Journal of Botany* 94:275–  
736 288. doi: 10.3732/ajb.94.3.275
- 737 Simmons MP, Ochoterena H (2000) Gaps as characters in sequence-based  
738 phylogenetic analyses. *Systematic Biology* 49:369–381.
- 739 Simpson BB (1975) Pleistocene changes in the flora of the high tropical Andes.  
740 *Paleobiology* 1:273–294. doi: 10.2307/2400369
- 741 Taberlet P, Gielly L, Pautou G, Bouvet J (1991) Universal primers for amplification  
742 of three non-coding regions of chloroplast DNA. *Plant Mol Biol* 17:1105–1109.
- 743 Tate JA, Simpson BB (2003) Paraphyly of *Tarasa* (Malvaceae) and diverse origins of  
744 the polyploid species. *Systematic Botany* 28:723–737. doi:  
745 10.2307/25063919?ref=search-gateway:ab20df06ffd5b47899780d1c7b361d21
- 746 Teacher AGF, Griffiths DJ (2011) HapStar: automated haplotype network layout and  
747 visualization. *Molecular Ecology Resources* 11:151–153. doi: 10.1111/j.1755-  
748 0998.2010.02890.x
- 749 Templeton AR (1998) Nested clade analyses of phylogeographic data: testing



750 hypotheses about gene flow and population history. *Mol Ecol* 7:381–397.

1 751 Tremetsberger K, Urtubey E, Terrab A, et al (2009) Pleistocene refugia and  
2 752 polytopic replacement of diploids by tetraploids in the Patagonian and  
3 753 Subantarctic plant *Hypochoeris incana* (Asteraceae, Cichorieae). *Mol Ecol*  
4 754 18:3668–3682. doi: 10.1111/j.1365-294X.2009.04298.x

6 755 van der Hammen T (1974) The Pleistocene changes of vegetation and climate in  
8 756 tropical South America. *Journal of Biogeography* 1:3–26.

10 757 van der Hammen T, Cleef AM (1986) Development of the high Andean Páramo flora  
11 758 and vegetation. In: Vuilleumier F, Monasterio M (eds) *High Altitude Tropical*  
12 759 *Biogeography*, First. Oxford University Press, Inc, New York, pp 153–201

14 760 Vásquez DLA, Balslev H, Hansen MM, et al (2016) Low genetic variation and high  
16 761 differentiation across sky island populations of *Lupinus alopecuroides*  
17 762 (Fabaceae) in the northern Andes. *Alpine Botany* 1–8. doi: 10.1007/s00035-016-  
18 763 0165-7

20 764 Wondimu T, Gizaw A, Tusiime FM, et al (2013) Crossing barriers in an extremely  
22 765 fragmented system: two case studies in the afro-alpine sky island flora. *Plant*  
23 766 *Syst Evol* 300:415–430. doi: 10.1007/s00606-013-0892-9

1  
2  
3  
4  
5  
6  
7  
8  
9  
10  
11  
12  
13  
14  
15  
16  
17  
18  
19  
20  
21  
22  
23  
24  
25  
26  
27  
28  
29  
30  
31  
32  
33  
34  
35  
36  
37  
38  
39  
40  
41  
42  
43  
44  
45  
46  
47  
48  
49  
50  
51  
52  
53  
54  
55  
56  
57  
58  
59  
60  
61  
62  
63  
64  
65

15  
16  
17  
18  
19  
20  
21  
22  
23  
24  
25  
26  
27  
28  
29  
30  
31  
32  
33  
34  
35  
36  
37  
38  
39  
40  
41  
42  
43  
44  
45  
46  
47  
48  
49  
50  
51  
52  
53  
54  
55  
56  
57  
58  
59  
60  
61  
62  
63  
64  
65

767 TABLES

Table 1. Molecular diversity indices for ITS and cpDNA (*trnL-F*, *trnH-psbA* and *rpl32-trnL*) for each species. N: number of individuals; H: number of haplotypes; hr: haplotype richness (ITS, rarefied to a minimum sample of 15; cpDNA, rarefied to a minimum sample of 9); h, haplotype diversity ( $\pm$  SD);  $\pi$ , nucleotide diversity ( $\pm$  SD). A, *O. obtusangulus* considered as one species; B, *O. obtusangulus* considered as two species.

Species	N	H	hr	h	$\pi \times 100$
<b>ITS</b>					
<i>O. cleefii</i>	15	5	5.00	0.70 $\pm$ 0.11	0.45 $\pm$ 0.30
<i>O. ecuadorensis</i>	24	4	3.12	0.31 $\pm$ 0.12	0.01 $\pm$ 0.10
<i>O. goeppingeri</i>	75	12	6.09	0.79 $\pm$ 0.03	1.15 $\pm$ 0.61
<i>O. obtusangulus</i>					
NA	23	8	6.12	0.68 $\pm$ 0.10	0.56 $\pm$ 0.35
SA	33	5	3.88	0.64 $\pm$ 0.06	2.25 $\pm$ 1.16
Combined	56	13	6.59	0.82 $\pm$ 0.03	2.76 $\pm$ 1.39
<i>O. venezuelensis</i>	27	7	5.02	0.63 $\pm$ 0.10	1.49 $\pm$ 0.80
<b>cpDNA</b>					
<i>O. cleefii</i>	9	4	4.00	0.78 $\pm$ 0.11	1.96 $\pm$ 1.07
<i>O. ecuadorensis</i>	29	5	3.54	0.72 $\pm$ 0.05	0.11 $\pm$ 0.07
<i>O. goeppingeri</i>	27	11	5.67	0.84 $\pm$ 0.06	2.36 $\pm$ 1.17
<i>O. obtusangulus</i>					
NA	20	10	6.35	0.91 $\pm$ 0.04	1.70 $\pm$ 0.86
SA	19	8	5.22	0.84 $\pm$ 0.06	2.20 $\pm$ 1.11
Combined	39	18	7.12	0.94 $\pm$ 0.02	3.05 $\pm$ 1.49
<i>O. venezuelensis</i>	14	8	6.30	0.91 $\pm$ 0.05	2.23 $\pm$ 1.15

Table 2. Pairwise  $F_{ST}$  values amongst species calculated from ITS and cpDNA (*trnL-F*, *trnH-psbA* and *rpl32-trnL*) considering *O. obtusangulus* as (a) one species and (b) as two species. Values for ITS are below the diagonal and cpDNA above. Bold numbers denote significance at the 5% level. cle: *O. cleefii*, ecu: *O. ecuadorensis*, goe: *O. goeppingeri*, obt: *O. obtusangulus* and ven: *O. venezuelensis*.

(a)

	cle	ecu	goe	obt	ven	
cle		<b>0.797</b>	<b>0.283</b>	<b>0.098</b>	<b>0.317</b>	cle
ecu	<b>0.770</b>		<b>0.732</b>	<b>0.600</b>	<b>0.801</b>	ecu
goe	<b>0.284</b>	<b>0.307</b>		<b>0.229</b>	<b>0.288</b>	goe
obt	<b>0.269</b>	<b>0.360</b>	<b>0.289</b>		<b>0.256</b>	obt
ven	<b>0.314</b>	<b>0.328</b>	<b>0.175</b>	<b>0.291</b>		ven
	cle	ecu	goe	obt	ven	

(b)

	cle	ecu	goe	obt (NA)	obt (SA)	ven	
cle		<b>0.797</b>	<b>0.283</b>	-0.020	<b>0.487</b>	<b>0.317</b>	cle
ecu	<b>0.770</b>		<b>0.732</b>	<b>0.780</b>	<b>0.819</b>	<b>0.801</b>	ecu
goe	<b>0.284</b>	<b>0.307</b>		<b>0.363</b>	<b>0.430</b>	<b>0.288</b>	goe
obt (NA)	<b>0.157</b>	<b>0.710</b>	<b>0.294</b>		<b>0.547</b>	<b>0.399</b>	obt (NA)
obt (SA)	<b>0.595</b>	<b>0.649</b>	<b>0.578</b>	<b>0.620</b>		<b>0.478</b>	obt (SA)
ven	<b>0.314</b>	<b>0.328</b>	<b>0.175</b>	<b>0.339</b>	<b>0.551</b>		ven
	cle	ecu	goe	obt (NA)	obt (SA)	ven	

Table 3. Analysis of molecular variance (AMOVA) results for ITS and cpDNA (*trnL-F*, *trnH-psbA* and *rpl32-trnL*).

Group level	Source of variation	Degrees of freedom		Sum of Squares		Variance components		Percentage of variation		Fixation indices	
		ITS	cpDNA	ITS	cpDNA	ITS	cpDNA	ITS	cpDNA	ITS	cpDNA
Species	Among species	4	4	260	2033	1.69	21.67	30.46	47.65	$F_{ST} = 0.31^{***}$	$F_{ST} = 0.48^{***}$
	Within species	192	113	741	2689	3.86	23.80	69.54	52.35		
Clusters (all clusters)	Among clusters	13	12	442	1925	2.30	15.54	42.95	36.84	$F_{ST} = 0.43^{***}$	$F_{ST} = 0.37^{***}$
	Within clusters	183	105	560	2798	3.06	26.65	57.05	63.16		
Clusters (northern Andes - NA)	Among clusters	9	8	88	885	0.46	7.88	14.50	21.34	$F_{ST} = 0.15^{**}$	$F_{ST} = 0.21^{***}$
	Within clusters	154	90	416	2612	2.70	29.03	85.50	78.66		
Continental regions (NA vs SA)	Among regions	1	1	309	746	5.38	19.89	59.49	35.54	$F_{CT} = 0.60^{***}$	$F_{CT} = 0.36^{***}$
	Among clusters within regions	12	11	133	1179	0.61	9.41	6.72	16.82	$F_{SC} = 0.17^{**}$	$F_{SC} = 0.26^{***}$
	Within clusters	183	105	560	2798	3.06	26.65	33.79	47.64	$F_{ST} = 0.66^{***}$	$F_{ST} = 0.52^{***}$
SAMOVA groups	Among groups	2	2	348	999	5.71	25.47	62.19	42.59	$F_{CT} = 0.62^{***}$	$F_{CT} = 0.43^{***}$
	Among clusters within groups	11	10	93	926	0.41	7.68	4.51	12.84	$F_{SC} = 0.12^*$	$F_{SC} = 0.22^{***}$
	Within clusters	183	105	560	2798	3.06	26.65	33.30	44.56	$F_{ST} = 0.67^{***}$	$F_{ST} = 0.55^{***}$

768 \* significant at the 5% level; \*\* significant at the 1% level; \*\*\* significant at the 0.1% level

Table 4. Molecular diversity indices for ITS and cpDNA (*trnL-F*, *trnH-psbA* and *rpl32-trnL*) for each SAMOVA grouping. N: number of individuals; H: number of haplotypes; hr: haplotype richness (ITS, rarefied to a minimum sample of 16; cpDNA, rarefied to a minimum sample of 9); h, haplotype diversity ( $\pm$  SD);  $\pi$ , nucleotide diversity ( $\pm$  SD).

SAMOVA group	N	H	hr	h	$\pi \times 100$
<i>ITS</i>					
I	164	25	9.20	0.91 $\pm$ 0.01	1.18 $\pm$ 0.63
II	17	5	4.88	0.58 $\pm$ 0.13	2.18 $\pm$ 1.17
III	16	2	2.00	0.13 $\pm$ 0.11	1.46 $\pm$ 0.80
<i>cpDNA</i>					
I	100	33	7.43	0.95 $\pm$ 0.01	3.03 $\pm$ 1.46
II	9	4	4.00	0.58 $\pm$ 0.18	1.90 $\pm$ 1.04
III	9	4	4.00	0.75 $\pm$ 0.11	0.06 $\pm$ 0.05

1  
2  
3  
4  
5  
6  
7  
8  
9  
10  
11  
12  
13  
14  
15  
16  
17  
18  
19  
20  
21  
22  
23  
24  
25  
26  
27  
28  
29  
30  
31  
32  
33  
34  
35  
36  
37  
38  
39  
40  
41  
42  
43  
44  
45  
46  
47  
48  
49  
50  
51  
52  
53  
54  
55  
56  
57  
58  
59  
60  
61  
62  
63  
64  
65

1 769 FIGURES  
2  
3  
4

5 770 **Fig. 1** Geographical distribution of *Oreobolus* in South America based on herbarium  
6  
7 771 records (coloured dots). Sampling localities (1 – 32) and their corresponding cluster  
8  
9 772 (A – N) are also indicated. Arrows denote geographical features.

10  
11  
12  
13 773 **Fig. 2** Maximum clade credibility tree from the \*BEAST 2 analysis based on ITS  
14  
15 774 and cpDNA (*trnL-F*, *trnH-psbA* and *rpl32-trnL*). Numbers above the branches  
16  
17  
18 775 represent posterior probability values. Node bars show 95% HPD. NAC, northern  
19  
20  
21 776 Andean clade.

22  
23  
24 777 **Fig. 3** NeighborNet network for the ITS haplotypes based on the uncorrected-p  
25  
26 778 distances. Haplotypes are coloured according to species. Shared haplotypes are  
27  
28  
29 779 shown in white, with pie charts below (labelled with haplotype number) showing the  
30  
31 780 frequency per species. NA: northern Andes, SA: southern Andes

32  
33  
34 781 **Fig. 4** NeighborNet network for the cpDNA (*trnL-F*, *trnH-psbA* and *rpl32-trnL*)  
35  
36 782 haplotypes based on the uncorrected-p distances. Haplotypes are coloured according  
37  
38  
39 783 to species. Shared haplotypes are shown in white, with pie charts (labelled with  
40  
41  
42 784 haplotype number) indicating frequency per species shown below. NA: northern  
43  
44 785 Andes, SA: southern Andes

45  
46  
47 786 **Fig. 5** NeighborNet network showing genetic relatedness amongst clusters based on  
48  
49 787 ITS and cpDNA (*trnL-F*, *trnH-psbA* and *rpl32-trnL*)  $F_{ST}$  pairwise values.  
50  
51  
52  
53  
54  
55  
56  
57  
58  
59  
60  
61  
62  
63  
64  
65

Supplementary Table 1. Geographic coordinates and corresponding cluster of the sampling localities.

Nº	SAMPLING LOCALITY	CLUSTER	LATITUDE	LONGITUDE
1	CHIRRIPO	A	9.48411000	-83.48861000
2	COCUY	B	6.41211667	-72.33128333
3	LA RUSIA	C	5.93951667	-73.07583333
4	IGUAQUE	C	5.68610000	-73.44773333
5	TOTA-BIJAGUAL	B	5.48143333	-72.85540000
6	RABANAL	C	5.40818333	-73.54915000
7	GUERRERO	C	5.22618333	-74.01788333
8	CHINGAZA	D	4.52848333	-73.75866667
9	SUMAPAZ	D	4.28958333	-74.20781667
10	PURACE	E	2.36088333	-76.35038333
11	AZUFRAL	F	1.09543333	-77.68711667
12	VOLCAN CHILES	F	0.80000000	-77.93333333
13	MIRADOR	F	0.56666667	-77.65000000
14	COTOCACHI	F	0.36666667	-78.33333333
15	COTOPAXI	G	-0.66666667	-78.36666667
16	LLANGANATI	G	-1.15000000	-78.30000000
17	ALAO-HUAMBOYA	G	-1.80000000	-78.43333333
18	PARAMO DE LAS CAJAS	H	-2.81666667	-79.26666667
19	CUENCA-LIMON	H	-3.00000000	-78.66666667
20	CUENCA-LOJA	H	-3.16666667	-79.03333333
21	PODOCARPUS	I	-4.40000000	-79.10000000
22	CAJAMARCA	J	-7.05000000	-78.58333333
23	HUASCARAN	J	-9.45000000	-77.26666000
24	VALDIVIA	K	-40.18333333	-73.51666666
25	FIORDO PEEL	L	-50.50000000	-73.73333333
26	MALVINAS	N	-51.64297000	-59.89473000
27	MORRO PHILIPPI	L	-51.73333333	-71.50000000
28	MAGALLANES	L	-53.45000000	-71.76666700
29	TIERRA DEL FUEGO	M	-54.76666666	-67.40000000
30	ISLA DE LOS ESTADOS	M	-54.80000000	-64.31666666
31	ISLA NAVARINO	M	-55.07553100	-67.65539600
32	CABO DE HORNOS	M	-55.94407800	-67.28092500

Supplementary Table 2. Sequence information

Supplementary Table 3. Number of individuals successfully sequenced per species per sampling locality for ITS and cpDNA (*trnL-F*, *trnH-psbA* and *rpl32-trnL*). Areas where species are not distributed are noted as n.d.

CLUSTER/Sampling locality	<i>O. cleefii</i>		<i>O. ecuadorensis</i>		<i>O. goeppingeri</i>		<i>O. obtusangulus</i>		<i>O. venezuelensis</i>	
	ITS	cpDNA	ITS	cpDNA	ITS	cpDNA	ITS	cpDNA	ITS	cpDNA
CLUSTER A										
(1) Chirripo	n.d.	n.d.	n.d.	n.d.	2	-	n.d.	n.d.	-	-
CLUSTER B										
(2) Cocuy	5	4	n.d.	n.d.	3	4	-	-	-	-
(5) Tota-Bijagual	2	1	n.d.	n.d.	2	1	-	-	-	-
CLUSTER C										
(4) Iguaque	-	-	n.d.	n.d.	1	1	-	-	-	-
(3) La Rusia	2	2	n.d.	n.d.	1	-	-	-	2	1
(6) Rabanal	-	-	n.d.	n.d.	2	1	-	-	-	-
(7) Guerrero	1	-	n.d.	n.d.	1	-	-	-	-	-
CLUSTER D										
(8) Chingaza	1	-	n.d.	n.d.	3	1	-	-	2	1
(9) Sumapaz	-	-	n.d.	n.d.	3	2	1	-	4	2
CLUSTER E										
(10) Purace	n.d.	n.d.	n.d.	n.d.	3	3	-	-	-	-
CLUSTER F										
(11) Azufral	4	2	-	-	1	1	-	-	-	-
(12) Volcan Chiles	-	-	1	1	5	-	5	4	-	-
(13) Mirador	-	-	-	-	2	2	1	2	1	1
(14) Cotocachi	n.d.	n.d.	1	2	3	2	-	-	-	-
CLUSTER G										
(15) Cotopaxi	n.d.	n.d.	9	13	2	-	2	2	-	1
(16) Llanganati	n.d.	n.d.	-	1	2	-	2	1	-	-



15  
16  
17  
18  
19  
20  
21  
22  
23  
24  
25  
26  
27  
28  
29  
30  
31  
32  
33  
34  
35  
36  
37  
38  
39  
40  
41  
42  
43  
44  
45  
46  
47  
48  
49  
50  
51  
52  
53  
54  
55  
56  
57  
58  
59  
60  
61  
62  
63  
64  
65

(17) Alao-Huamboya	n.d.	n.d.	3	2	3	-	-	-	-	-
CLUSTER H										
(18) Paramo De Las Cajas	n.d.	n.d.	3	4	2	2	4	3	-	-
(19) Cuenca-Limon	n.d.	n.d.	-	-	2	-	3	3	-	-
(20) Cuenca-Loja	n.d.	n.d.	4	4	11	3	3	3	2	3
CLUSTER I										
(21) Podocarpus	n.d.	n.d.	-	-	18	4	1	1	15	4
CLUSTER J										
(22) Cajamarca	n.d.	n.d.	1	1	3	-	1	1	-	-
(23) Huascan	n.d.	n.d.	2	1	-	-	-	-	-	-
CLUSTER K										
(24) Valdivia	n.d.	n.d.	n.d.	n.d.	n.d.	n.d.	1	1	n.d.	n.d.
CLUSTER L										
(25) Fiordo Peel	n.d.	n.d.	n.d.	n.d.	n.d.	n.d.	2	-	n.d.	n.d.
(27) Morro Philippi	n.d.	n.d.	n.d.	n.d.	n.d.	n.d.	2	1	n.d.	n.d.
(28) Magallanes	n.d.	n.d.	n.d.	n.d.	n.d.	n.d.	11	7	n.d.	n.d.
CLUSTER M										
(29) Tierra Del Fuego	n.d.	n.d.	n.d.	n.d.	n.d.	n.d.	10	5	n.d.	n.d.
(30) Isla De Los Estados	n.d.	n.d.	n.d.	n.d.	n.d.	n.d.	2	1	n.d.	n.d.
(31) Isla Navarino	n.d.	n.d.	n.d.	n.d.	n.d.	n.d.	1	-	n.d.	n.d.
(32) Cabo De Hornos	n.d.	n.d.	n.d.	n.d.	n.d.	n.d.	3	3	n.d.	n.d.
CLUSTER N										
(26) Malvinas	n.d.	n.d.	n.d.	n.d.	n.d.	n.d.	1	1	n.d.	n.d.
TOTAL	15	9	24	29	75	27	56	39	27	14





1  
2  
3  
4  
5  
6  
7  
8  
9  
10  
11  
12  
13  
14  
15  
16  
17  
18  
19  
20  
21  
22  
23  
24  
25  
26  
27  
28  
29  
30  
31  
32  
33  
34  
35  
36  
37  
38  
39  
40  
41  
42  
43  
44  
45  
46  
47  
48  
49  
50  
51  
52  
53  
54  
55  
56  
57  
58  
59  
60  
61  
62  
63  
64  
65

	<i>ecu</i>	.	.	.	.	.	.	.	.	.	.	.	.	.	.
	<i>goe</i>	.	.	.	.	.	.	.	.	.	.	.	.	.	.
	<i>obt</i>	.	.	.	.	.	.	.	.	.	.	1	.	.	.
	<i>ven</i>	.	.	.	.	.	.	.	.	.	.	.	.	.	.
	<i>cle</i>	.	.	.	.	.	.	.	.	.	.	.	.	.	.
Hn24	<i>ecu</i>	.	.	.	.	.	.	.	.	.	.	.	.	.	.
	<i>goe</i>	.	.	.	.	.	.	.	.	.	.	.	.	.	.
	<i>obt</i>	.	.	.	.	.	3	2	8	.	.	.	.	.	.
	<i>ven</i>	.	.	.	.	.	.	.	.	.	.	.	.	.	.
	<i>cle</i>	.	.	.	.	.	.	.	.	.	.	.	.	.	.
	<i>ecu</i>	.	.	.	.	.	.	.	.	.	.	.	.	.	.
Hn25	<i>goe</i>	.	.	.	.	.	.	.	.	.	.	.	2	.	.
	<i>obt</i>	.	.	.	.	.	.	.	.	.	.	.	.	.	.
	<i>ven</i>	.	.	.	.	.	.	.	.	.	.	.	.	.	.
	<i>cle</i>	.	.	.	.	.	.	.	.	.	.	.	.	.	.
	<i>ecu</i>	.	.	.	.	.	.	.	.	.	.	.	.	.	.
Hn26	<i>goe</i>	.	.	.	.	.	.	.	.	.	.	.	.	.	.
	<i>obt</i>	.	.	.	.	.	.	.	.	.	.	.	.	.	.
	<i>ven</i>	.	.	1	.	.	.	.	.	.	.	.	.	.	.
	<i>cle</i>	.	.	.	.	.	.	.	.	.	.	.	.	.	.
	<i>ecu</i>	.	.	.	.	.	.	.	.	.	.	.	.	.	.
Hn27	<i>goe</i>	.	.	.	.	.	.	.	.	.	.	.	.	.	.
	<i>obt</i>	.	.	.	.	.	.	.	.	.	.	.	.	.	.
	<i>ven</i>	.	.	.	1	.	.	.	.	.	.	.	.	.	.
	<i>cle</i>	.	.	.	.	.	.	.	.	.	.	.	.	.	.
	<i>ecu</i>	.	.	.	.	.	.	.	.	.	.	.	.	.	.
Hn28	<i>goe</i>	.	.	.	.	.	.	.	.	.	.	.	.	.	.
	<i>obt</i>	.	.	.	.	.	.	.	.	.	.	.	.	.	.
	<i>ven</i>	.	.	.	.	.	.	.	1	15	.	.	.	.	.
	<i>cle</i>	.	.	.	.	.	.	.	.	.	.	.	.	.	.
	<i>ecu</i>	.	.	.	.	.	.	.	.	.	.	.	.	.	.
Hn29	<i>goe</i>	.	.	.	.	.	.	.	.	.	.	.	.	.	.
	<i>obt</i>	.	.	.	.	.	.	.	.	.	.	.	.	.	.
	<i>ven</i>	.	.	.	1	.	.	.	.	.	.	.	.	.	.
	<i>cle</i>	.	.	.	.	.	.	.	.	.	.	.	.	.	.
	<i>ecu</i>	.	.	.	.	.	.	.	.	.	.	.	.	.	.
Hn30	<i>goe</i>	.	.	.	.	.	.	.	.	.	.	.	.	.	.
	<i>obt</i>	.	.	.	.	.	.	.	.	.	.	.	.	.	.
	<i>ven</i>	.	.	.	.	.	.	.	1	.	.	.	.	.	.



1  
2  
3  
4  
5  
6  
7  
8  
9  
10  
11  
12  
13  
14  
15  
16  
17  
18  
19  
20  
21  
22  
23  
24  
25  
26  
27  
28  
29  
30  
31  
32  
33  
34  
35  
36  
37  
38  
39  
40  
41  
42  
43  
44  
45  
46  
47  
48  
49  
50  
51  
52  
53  
54  
55  
56  
57  
58  
59  
60  
61  
62  
63  
64  
65

Hc11	<i>cle</i>	.	.	.	.	.	.	.	.	.	.	.	.	.
	<i>ecu</i>	.	.	.	.	.	.	.	.	.	.	.	.	.
	<i>goe</i>	.	.	.	.	2	.	2	.	.	.	.	.	.
	<i>obt</i>	.	.	.	.	.	.	.	.	.	.	.	.	.
Hc12	<i>ven</i>	.	.	.	.	.	.	.	.	.	.	.	.	.
	<i>cle</i>	.	.	.	.	.	.	.	.	.	.	.	.	.
	<i>ecu</i>	.	.	.	.	.	.	.	.	.	.	.	.	.
	<i>goe</i>	2	1	2	.	2	.	3	.	.	.	.	.	.
Hc13	<i>obt</i>	.	.	.	.	.	.	.	.	.	.	.	.	.
	<i>ven</i>	.	.	.	.	.	.	.	.	.	.	.	.	.
	<i>cle</i>	.	.	.	.	.	.	.	.	.	.	.	.	.
	<i>ecu</i>	.	.	.	.	.	.	.	.	.	.	.	.	.
Hc14	<i>goe</i>	1	.	1	1	.	.	.	.	.	.	.	.	.
	<i>obt</i>	.	.	.	.	.	.	.	.	.	.	.	.	.
	<i>ven</i>	.	1	2	.	.	.	.	.	.	.	.	.	.
	<i>cle</i>	.	.	.	.	.	.	.	.	.	.	.	.	.
Hc15	<i>ecu</i>	.	.	.	.	.	.	.	.	.	.	.	.	.
	<i>goe</i>	2	.	.	.	.	.	.	.	.	.	.	.	.
	<i>obt</i>	.	.	.	.	.	.	.	.	.	.	.	.	.
	<i>ven</i>	.	.	1	.	.	.	.	.	.	.	.	.	.
Hc16	<i>cle</i>	.	.	.	.	.	.	.	.	.	.	.	.	.
	<i>ecu</i>	.	.	.	.	.	.	.	.	.	.	.	.	.
	<i>goe</i>	.	.	.	1	.	.	.	.	.	.	.	.	.
	<i>obt</i>	.	.	.	.	.	.	.	.	.	.	.	.	.
Hc17	<i>ven</i>	.	.	.	.	.	.	.	.	.	.	.	.	.
	<i>cle</i>	.	.	.	.	.	.	.	.	.	.	.	.	.
	<i>ecu</i>	.	.	.	.	.	.	.	.	.	.	.	.	.
	<i>goe</i>	.	.	.	.	1	.	.	.	.	.	.	.	.
Hc18	<i>obt</i>	.	.	.	.	.	.	.	.	.	.	.	.	.
	<i>ven</i>	.	.	.	.	.	.	.	.	.	.	.	.	.
	<i>cle</i>	.	.	.	.	.	.	.	.	.	.	.	.	.
	<i>ecu</i>	.	.	.	.	.	.	.	.	.	.	.	.	.
Hc19	<i>goe</i>	.	1	.	.	.	.	.	.	.	.	.	.	.
	<i>obt</i>	.	.	.	.	.	.	.	.	.	.	.	.	.
	<i>ven</i>	.	.	.	.	.	.	.	.	.	.	.	.	.
	<i>cle</i>	.	.	.	.	.	.	.	.	.	.	.	.	.
Hc20	<i>ecu</i>	.	.	.	.	.	.	.	.	.	.	.	.	.
	<i>goe</i>	.	.	.	.	.	.	.	2	.	.	.	.	.
	<i>obt</i>	.	.	.	.	.	.	.	.	.	.	.	.	.
	<i>ven</i>	.	.	.	.	.	.	.	.	.	.	.	.	.
Hc21	<i>cle</i>	.	.	.	.	.	.	.	.	.	.	.	.	.
	<i>ecu</i>	.	.	.	.	.	.	.	.	.	.	.	.	.
	<i>goe</i>	.	.	.	.	.	.	.	.	.	.	.	.	.
	<i>obt</i>	.	.	.	.	.	.	.	.	.	.	.	.	.
Hc22	<i>ven</i>	.	.	.	.	.	.	.	.	.	.	.	.	.
	<i>cle</i>	.	.	.	.	.	.	.	.	.	.	.	.	.
	<i>ecu</i>	.	.	.	.	.	.	.	.	.	.	.	.	.
	<i>goe</i>	.	.	.	.	.	.	.	.	.	.	.	.	.
	<i>obt</i>	.	.	.	.	.	.	.	.	.	1	.	.	.
	<i>ven</i>	.	.	.	.	.	.	.	.	.	.	.	.	.
	<i>cle</i>	.	.	.	.	.	.	.	.	.	.	.	.	.
	<i>ecu</i>	.	.	.	.	.	.	.	.	.	.	.	.	.

1  
2  
3  
4  
5  
6  
7  
8  
9  
10  
11  
12  
13  
14  
15  
16  
17  
18  
19  
20  
21  
22  
23  
24  
25  
26  
27  
28  
29  
30  
31  
32  
33  
34  
35  
36  
37  
38  
39  
40  
41  
42  
43  
44  
45  
46  
47  
48  
49  
50  
51  
52  
53  
54  
55  
56  
57  
58  
59  
60  
61  
62  
63  
64  
65

Hc23	cle	.	.	.	.	.	.	.	.	.	.	.	.	.	.
	ecu	.	.	.	.	.	.	.	.	.	.	.	.	.	.
	goe	.	.	.	.	.	.	.	.	.	.	.	.	.	.
	obt	.	.	.	.	.	.	.	.	.	.	.	.	1	.
	ven	.	.	.	.	.	.	.	.	.	.	.	.	.	.
Hc24	cle	.	.	.	.	.	.	.	.	.	.	.	.	.	.
	ecu	.	.	.	.	.	.	.	.	.	.	.	.	.	.
	goe	.	.	.	.	.	.	.	.	.	.	.	.	.	.
	obt	.	.	.	.	.	.	1	.	.	.	.	.	.	.
	ven	.	.	.	.	1	.	.	.	.	.	.	.	.	.
Hc25	cle	.	.	.	.	.	.	.	.	.	.	.	.	.	.
	ecu	.	.	.	.	.	.	.	.	.	.	.	.	.	.
	goe	.	.	.	.	.	.	.	.	.	.	.	.	.	.
	obt	.	.	.	.	.	.	.	1	.	.	.	.	.	.
	ven	.	.	.	.	.	.	.	.	.	.	.	.	.	.
Hc26	cle	.	.	.	.	.	.	.	.	.	.	.	.	.	.
	ecu	.	.	.	.	.	.	.	.	.	.	.	.	.	.
	goe	.	.	.	.	.	.	.	.	.	.	.	.	.	.
	obt	.	.	.	.	.	.	.	.	.	.	.	.	1	.
	ven	.	.	.	.	.	.	.	.	.	.	.	.	.	.
Hc27	cle	.	.	.	.	.	.	.	.	.	.	.	.	.	.
	ecu	.	.	.	.	.	.	.	.	.	.	.	.	.	.
	goe	.	.	.	.	.	.	.	.	.	.	.	.	.	.
	obt	.	.	.	.	.	1	2	2	.	.	.	.	.	.
	ven	.	.	.	.	.	.	.	.	.	.	.	.	.	.
Hc28	cle	.	.	.	.	.	.	.	.	.	.	.	.	.	.
	ecu	.	.	.	.	.	.	.	.	.	.	.	.	.	.
	goe	.	.	.	.	.	.	.	.	.	.	.	.	.	.
	obt	.	.	.	.	.	.	.	.	1	.	.	.	.	.
	ven	.	.	.	.	.	.	.	.	.	.	.	.	.	.
Hc29	cle	.	.	.	.	.	.	.	.	.	.	.	.	.	.
	ecu	.	.	.	.	.	.	.	.	.	.	.	.	.	.
	goe	.	.	.	.	.	.	.	.	.	.	.	.	.	.
	obt	.	.	.	.	.	.	.	.	1	.	.	.	.	.
	ven	.	.	.	.	.	.	.	.	.	.	.	.	.	.
Hc30	cle	.	.	.	.	.	.	.	.	.	.	.	.	.	.
	ecu	.	.	.	.	.	.	.	.	.	.	.	.	.	.
	goe	.	.	.	.	.	.	.	.	.	.	.	.	.	.
	obt	.	.	.	.	.	.	.	.	1	.	.	.	.	.
	ven	.	.	.	.	.	.	.	.	.	.	.	.	.	.
Hc31	cle	.	.	.	.	.	.	.	.	.	.	.	.	.	.
	ecu	.	.	.	.	.	.	.	.	.	.	.	.	.	.
	goe	.	.	.	.	.	.	.	.	.	.	.	.	.	.
	obt	.	.	.	.	.	.	.	.	2	.	.	.	.	.
	ven	.	.	.	.	.	.	.	.	.	.	.	.	.	.
Hc32	cle	.	.	.	.	.	.	.	.	.	.	.	.	.	.
	ecu	.	.	.	.	.	.	.	.	.	.	.	.	.	.
	goe	.	.	.	.	.	.	.	.	.	.	.	.	.	.
	obt	.	.	.	.	.	2	.	.	.	.	.	.	.	.
	ven	.	.	.	.	.	.	.	.	.	.	.	.	.	.
Hc33	cle	.	.	.	.	.	.	.	.	.	.	.	.	.	.
	ecu	.	.	.	.	.	.	.	.	.	.	.	.	.	.
	goe	.	.	.	.	.	.	.	.	.	.	.	.	.	.
	obt	.	.	.	.	.	.	.	.	.	.	.	.	3	.
	ven	.	.	.	.	.	.	.	.	.	.	.	.	.	.
Hc34	cle	.	.	.	.	.	.	.	.	.	.	.	.	.	.
	ecu	.	.	.	.	.	.	.	.	.	.	.	.	.	.
	goe	.	.	.	.	.	.	.	.	.	.	.	.	.	.
	obt	.	.	.	.	.	.	.	.	.	.	.	.	1	.
	ven	.	.	.	.	.	.	.	.	.	.	.	.	.	.

1  
2  
3  
4  
5  
6  
7  
8  
9  
10  
11  
12  
13  
14  
15  
16  
17  
18  
19  
20  
21  
22  
23  
24  
25  
26  
27  
28  
29  
30  
31  
32  
33  
34  
35  
36  
37  
38  
39  
40  
41  
42  
43  
44  
45  
46  
47  
48  
49  
50  
51  
52  
53  
54  
55  
56  
57  
58  
59  
60  
61  
62  
63  
64  
65

Hc35	<i>cle</i>	.	.	.	.	.	.	.	.	.	.	.	.	.
	<i>ecu</i>	.	.	.	.	.	.	.	.	.	.	.	.	.
	<i>goe</i>	.	.	.	.	.	.	.	.	.	.	.	.	.
	<i>obt</i>	.	.	.	.	.	.	.	.	.	.	.	1	.
Hc36	<i>cle</i>	.	.	.	.	.	.	.	.	.	.	.	.	.
	<i>ecu</i>	.	.	.	.	.	.	.	.	.	.	.	.	.
	<i>goe</i>	.	.	.	.	.	.	.	.	.	.	.	.	.
	<i>obt</i>	.	.	.	.	.	.	.	.	.	.	.	.	.
Hc37	<i>cle</i>	.	.	.	.	.	.	.	.	.	.	.	.	.
	<i>ecu</i>	.	.	.	.	.	.	.	.	.	.	.	.	.
	<i>goe</i>	.	.	.	.	.	.	.	.	.	.	.	.	.
	<i>obt</i>	.	.	.	.	.	.	.	.	.	.	.	.	.
Hc38	<i>cle</i>	.	.	.	.	.	.	.	.	.	.	.	.	.
	<i>ecu</i>	.	.	.	.	.	.	.	.	.	.	.	.	.
	<i>goe</i>	.	.	.	.	.	.	.	.	.	.	.	.	.
	<i>obt</i>	.	.	.	.	.	.	.	.	.	.	.	.	.
Hc39	<i>cle</i>	.	.	.	.	.	.	.	.	.	.	.	.	.
	<i>ecu</i>	.	.	.	.	.	.	.	.	.	.	.	.	.
	<i>goe</i>	.	.	.	.	.	.	.	.	.	.	.	.	.
	<i>obt</i>	.	.	.	.	.	.	.	.	.	.	.	.	.
Hc40	<i>cle</i>	.	.	.	.	.	.	.	.	.	.	.	.	.
	<i>ecu</i>	.	.	.	.	.	.	.	.	.	.	.	.	.
	<i>goe</i>	.	.	.	.	.	.	.	.	.	.	.	.	.
	<i>obt</i>	.	.	.	.	.	.	.	.	.	.	.	.	.
	<i>ven</i>	.	.	.	.	.	.	.	.	.	.	.	.	.



Supplementary Table 6. Spatial analysis of molecular variance (SAMOVA) results for ITS and cpDNA (*trnL-F*, *trnH-psbA* and *rpl32-trnL*) showing the variance amongst groups ( $F_{CT}$  values) for pre-defined K number of groups.

	K											
	2	3	4	5	6	7	8	9	10	11	12	13
$F_{CT}$ ITS	0.595	0.622	0.608	0.608	0.603	0.581	0.505	0.507	0.468	0.481	0.504	0.639
$F_{CT}$ cpDNA	0.417	0.426	0.417	0.414	0.412	0.406	0.405	0.410	0.441	0.502	0.675	-

1  
2  
3  
4  
5  
6  
7  
8  
9  
10  
11  
12  
13  
14  
15  
16  
17  
18  
19  
20  
21  
22  
23  
24  
25  
26  
27  
28  
29  
30  
31  
32  
33  
34  
35  
36  
37  
38  
39  
40  
41  
42  
43  
44  
45  
46  
47  
48  
49  
50  
51  
52  
53  
54  
55  
56  
57  
58  
59  
60  
61  
62  
63  
64  
65



Supplementary Table 8. Molecular diversity indices for ITS and cpDNA (*trnL-F*, *trnH-psbA* and *rpl32-trnL*) for each cluster. Clusters (A – N) as described in Figure 1 and Supplementary Table 1. Metrics were not applicable (n.a.) for clusters with less than three individuals. N, number of individuals; h, haplotype diversity ( $\pm$  SD);  $\pi$ , nucleotide diversity ( $\pm$  SD).

	ITS				cpDNA			
	SAMOVA group	N	h	$\pi \times 100$	SAMOVA group	N	h	$\pi \times 100$
A	I	2	n.a.	n.a.	-	-	-	-
B	I	13	0.69 $\pm$ 0.12	0.76 $\pm$ 0.46	I	10	0.82 $\pm$ 0.10	2.34 $\pm$ 1.25
C	I	10	0.82 $\pm$ 0.10	2.95 $\pm$ 1.63	I	5	0.90 $\pm$ 0.16	3.95 $\pm$ 2.41
D	I	14	0.85 $\pm$ 0.07	0.63 $\pm$ 0.39	I	6	0.73 $\pm$ 0.16	2.78 $\pm$ 1.62
E	I	3	0.67 $\pm$ 0.31	0.72 $\pm$ 0.63	I	3	1.00 $\pm$ 0.27	2.15 $\pm$ 1.62
F	I	24	0.86 $\pm$ 0.04	0.67 $\pm$ 0.40	I	17	0.93 $\pm$ 0.04	2.68 $\pm$ 1.36
G	I	23	0.76 $\pm$ 0.08	0.66 $\pm$ 0.40	I	20	0.77 $\pm$ 0.08	1.69 $\pm$ 0.86
H	I	34	0.83 $\pm$ 0.03	0.84 $\pm$ 0.48	I	25	0.92 $\pm$ 0.03	3.10 $\pm$ 1.55
I	I	34	0.67 $\pm$ 0.05	1.88 $\pm$ 0.98	I	10	0.91 $\pm$ 0.08	2.20 $\pm$ 1.18
J	I	7	0.91 $\pm$ 0.10	0.56 $\pm$ 0.39	I	3	0.67 $\pm$ 0.31	0.09 $\pm$ 0.08
K	II	1	n.a.	n.a.	I	1	n.a.	n.a.
L	II	15	0.55 $\pm$ 0.14	2.36 $\pm$ 1.27	II	8	0.64 $\pm$ 0.18	2.13 $\pm$ 1.18
M	III	16	0.13 $\pm$ 0.11	1.46 $\pm$ 0.80	III	9	0.75 $\pm$ 0.11	0.06 $\pm$ 0.05
N	II	1	n.a.	n.a.	II	1	n.a.	n.a.

1  
2  
3  
4  
5  
6  
7  
8  
9  
10  
11  
12  
13  
14  
15  
16  
17  
18  
19  
20  
21  
22  
23  
24  
25  
26  
27  
28  
29  
30  
31  
32  
33  
34  
35  
36  
37  
38  
39  
40  
41  
42  
43  
44  
45  
46  
47  
48  
49  
50  
51  
52  
53  
54  
55  
56  
57  
58  
59  
60  
61  
62  
63  
64  
65

795 **Supplementary Fig. 1** MST and distribution of ITS haplotypes. Numbers refer to  
796 haplotypes listed in Supplementary Table 5. Haplotypes are coloured according to  
797 species. Shared haplotypes are shown in white. Detail of species sharing haplotypes  
798 is given in Fig. 3. Hypothetical haplotypes are represented by filled black circles.  
799 Letters on the map refer to clusters as described in Figure 1 and Supplementary  
800 Table 3. Pie charts are proportional to sample size for each cluster (N = 1 – 34).  
801 Numbers next to each segment refer to haplotype number. NA: northern Andes, SA:  
802 southern Andes

803 **Supplementary Fig. 2** MST and distribution of cpDNA (*trnL-F*, *trnH-psbA* and  
804 *rpl32-trnL*) haplotypes. Numbers refer to haplotypes listed in Supplementary Table  
805 6. Haplotypes are coloured according to species. Shared haplotypes are shown in  
806 white. Detail of species sharing haplotypes is given in Fig. 5. Hypothetical  
807 haplotypes are represented by filled black circles, numbers within indicate their  
808 number when more than one. Letters on the map refer to clusters as described in  
809 Figure 1 and Supplementary Table 3. Pie charts are proportional to sample size for  
810 each cluster (N = 1 – 25). Numbers next to each segment refer to haplotype number.  
811 NA: northern Andes, SA: southern Andes

812 **Supplementary Fig. 3** NeighborNet network showing genetic relatedness amongst  
813 the South American species of *Oreobolus* based on ITS  $F_{ST}$  pairwise values  
814 considering (a) *O. obtusangulus* as one species (b) *O. obtusangulus* as two species  
815 **Supplementary Fig. 4** NeighborNet network showing genetic relatedness amongst  
816 the South American species of *Oreobolus* based on cpDNA (*trnL-F*, *trnH-psbA* and

817 *rpl32-trnL*) F<sub>ST</sub> pairwise values considering (a) *O. obtusangulus* as one species (b)

818 *O. obtusangulus* as two species

1  
2  
3  
4  
5  
6  
7  
8  
9  
10  
11  
12  
13  
14  
15  
16  
17  
18  
19  
20  
21  
22  
23  
24  
25  
26  
27  
28  
29  
30  
31  
32  
33  
34  
35  
36  
37  
38  
39  
40  
41  
42  
43  
44  
45  
46  
47  
48  
49  
50  
51  
52  
53  
54  
55  
56  
57  
58  
59  
60  
61  
62  
63  
64  
65

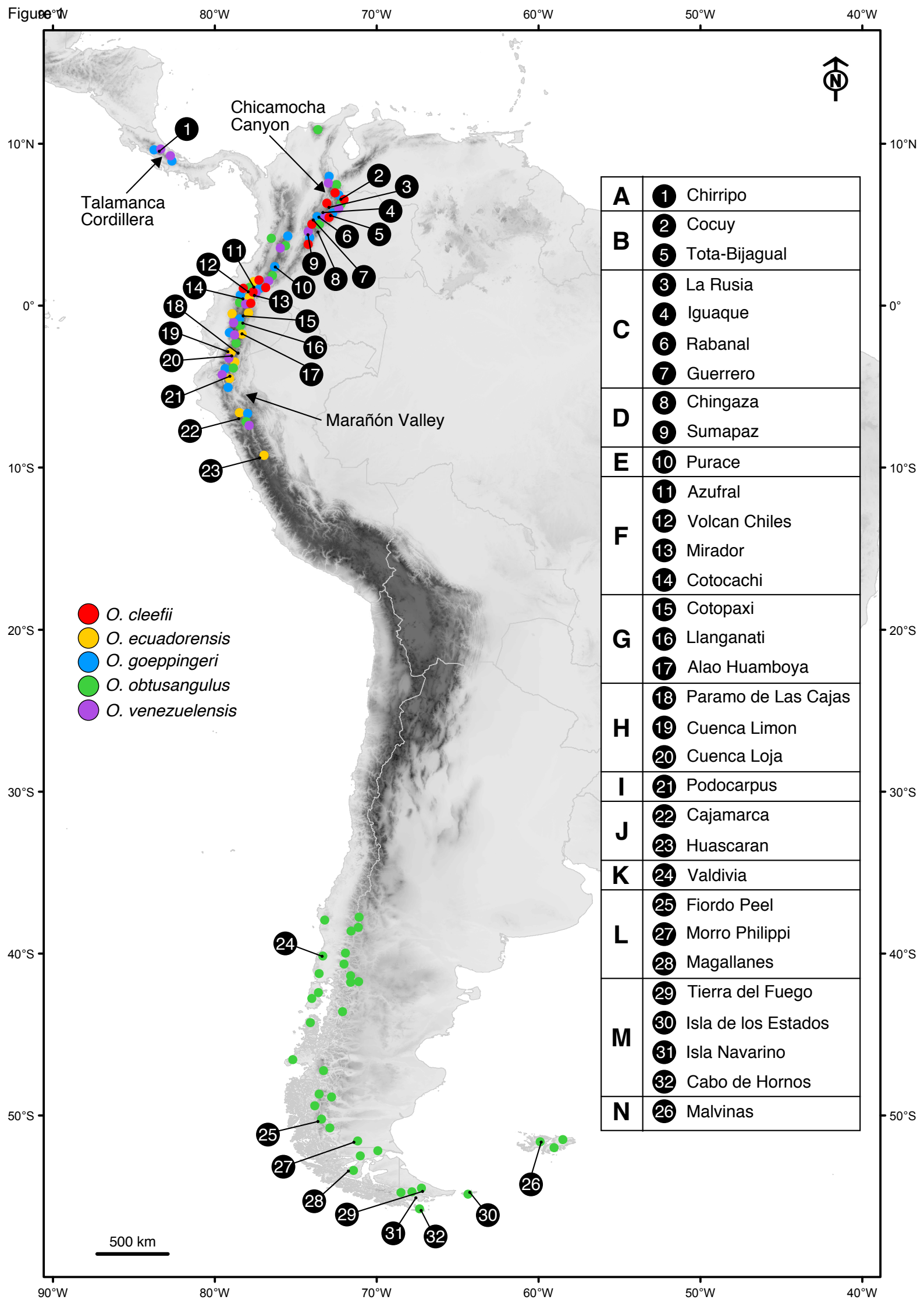


Figure 2

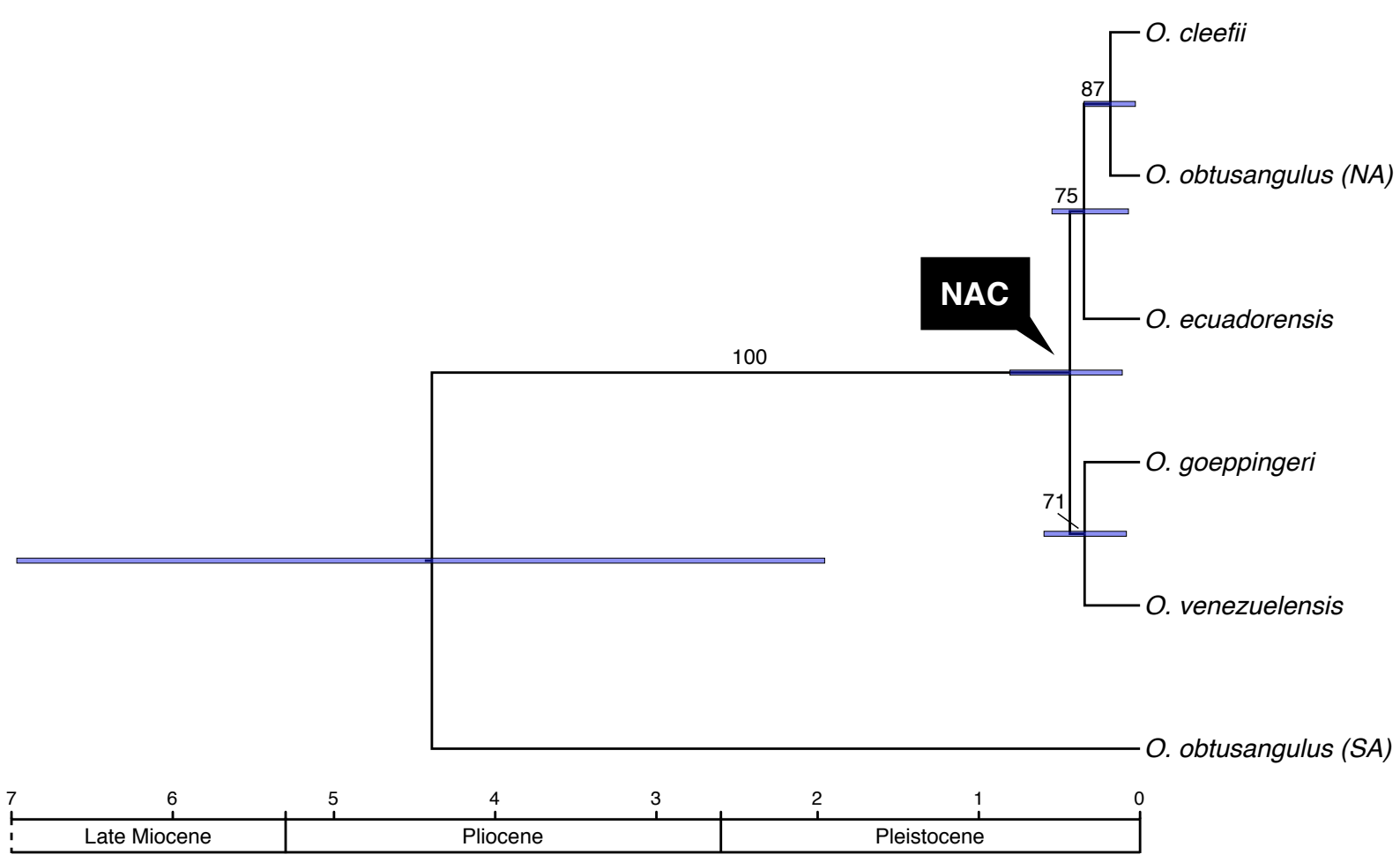
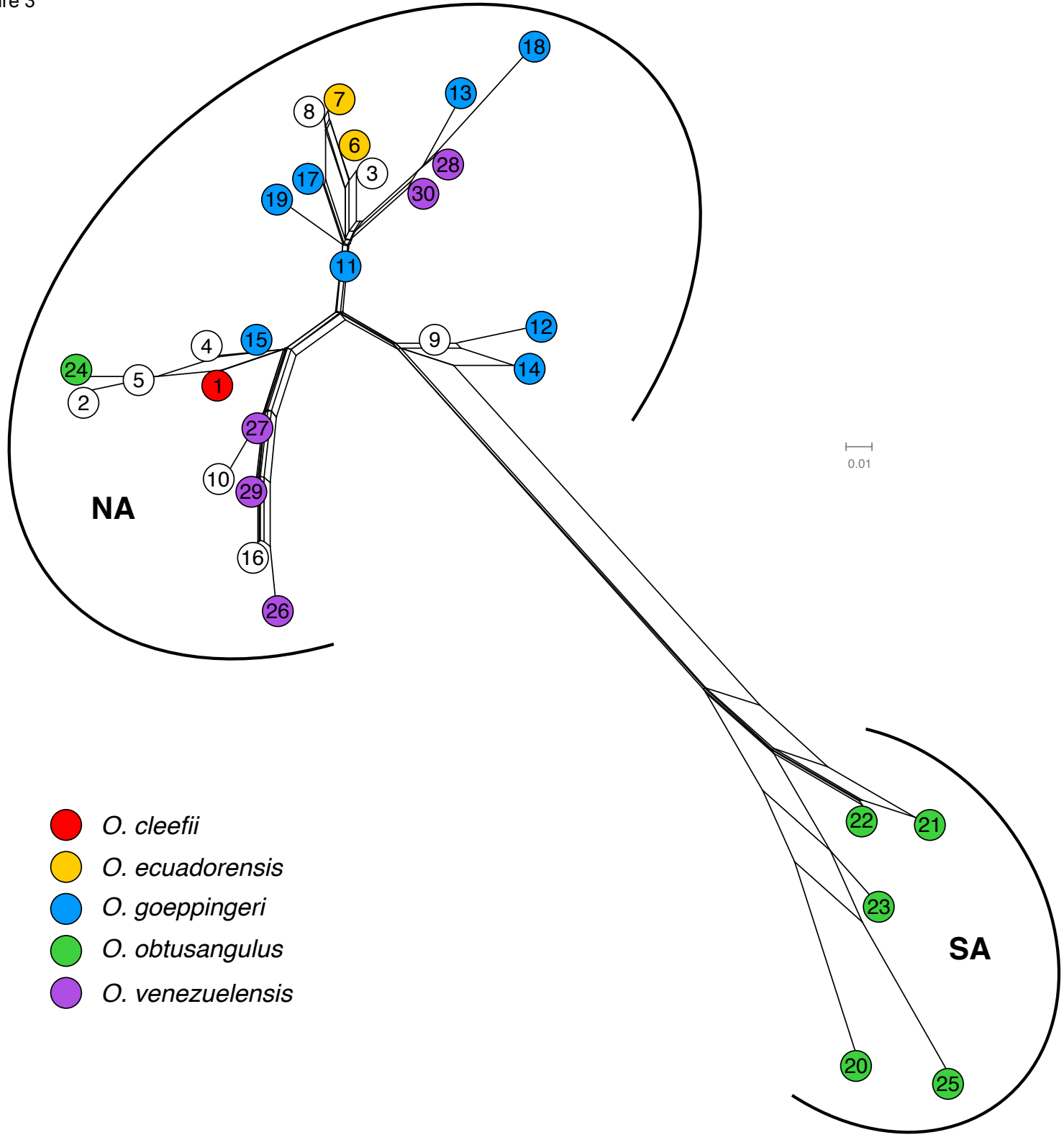


Figure 3



- O. cleefii*
- O. ecuadorensis*
- O. goeppingeri*
- O. obtusangulus*
- O. venezuelensis*

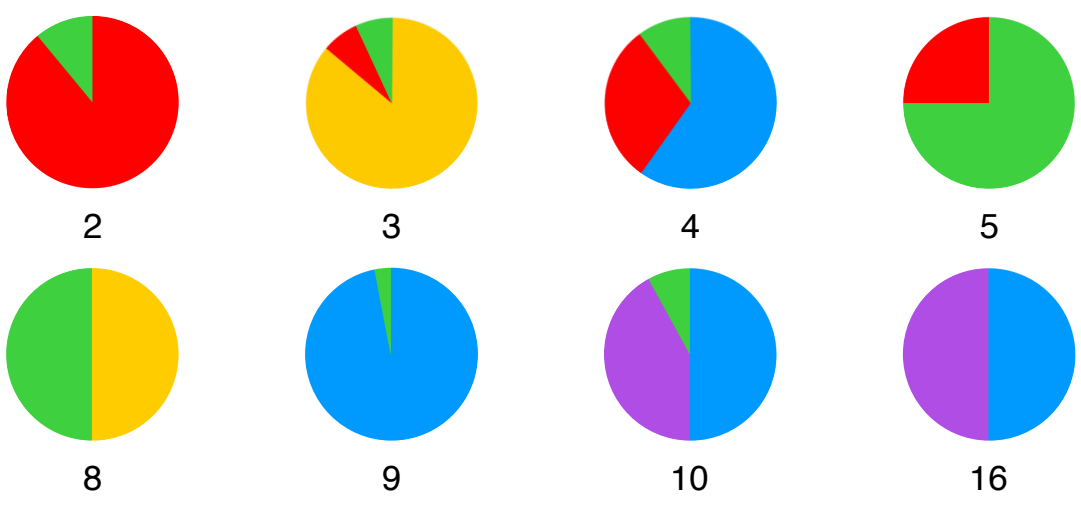
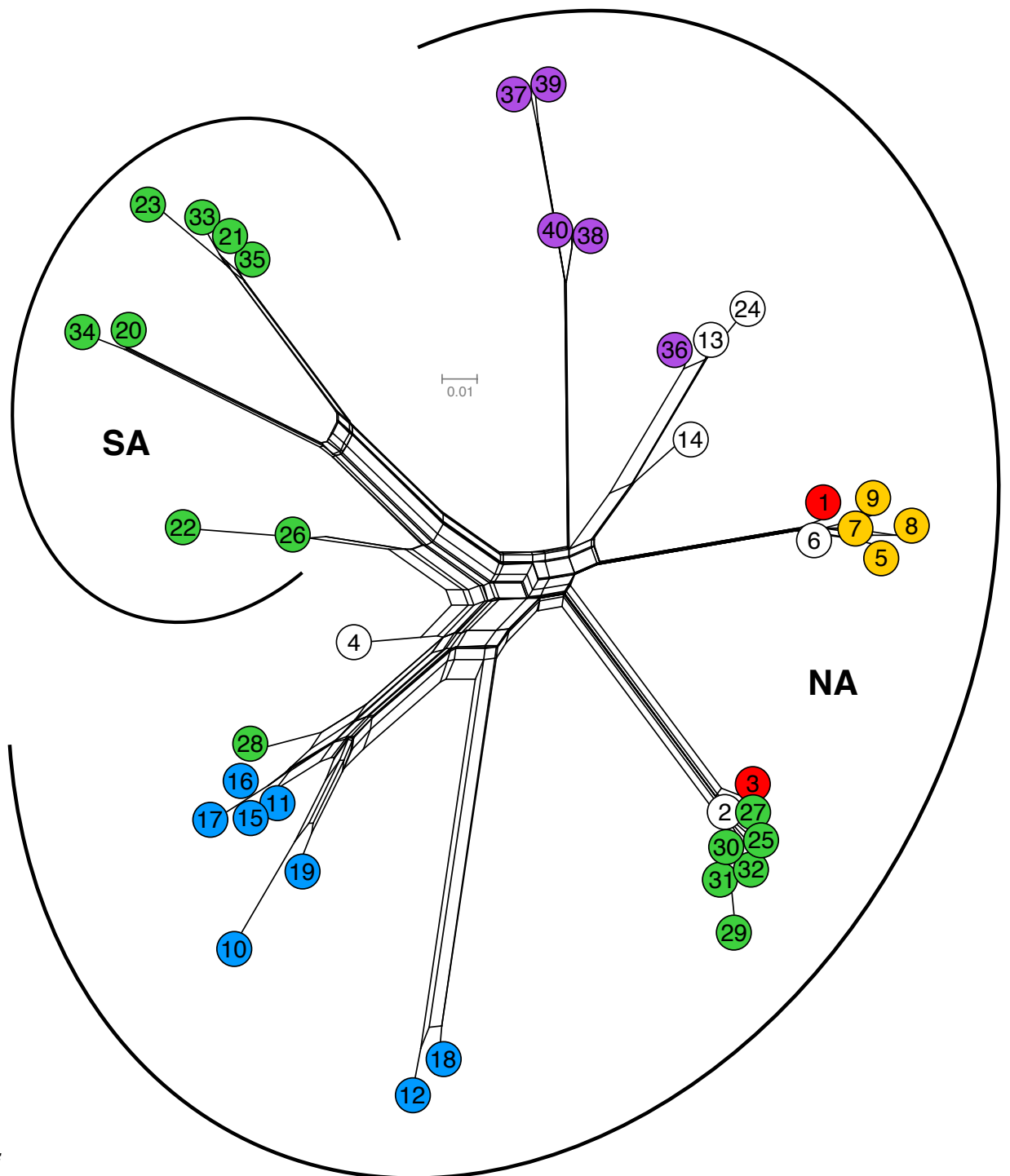
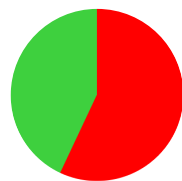




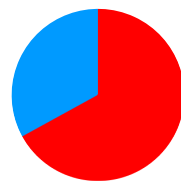
Figure 4



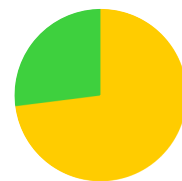
- *O. cleefii*
- *O. ecuadorensis*
- *O. goeppingeri*
- *O. obtusangulus*
- *O. venezuelensis*



2



4



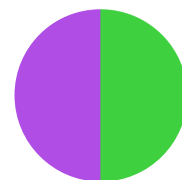
6



13



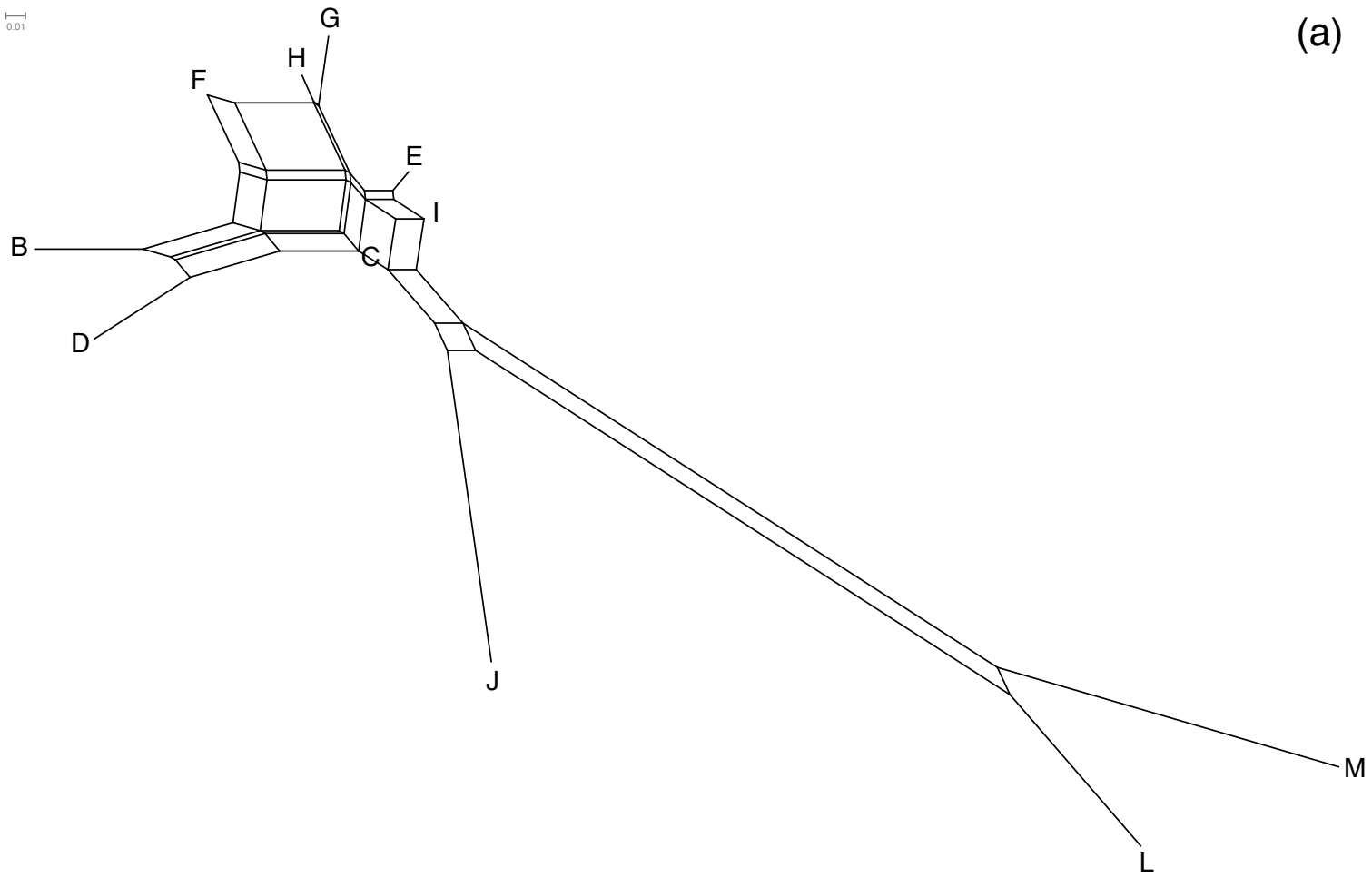
14



24

Figure 5

0.01



0.01

